ASTRONOMY & ASTROPHYSICS
SUPPLEMENT SERIES

Astron. Astrophys. Suppl. Ser. **99**, 513-543 (1993)

The hydrogen spectrum of model prominences

P. Gouttebroze[1], P. Heinzel[2] and J.C. Vial[1]

[1] Institut d'Astrophysique Spatiale, Université Paris XI, Bâtiment 121, 91405 Orsay Cedex, France
[2] Astronomical Institute, 25165 Ondřejov, Czechoslovakia

Received July 15; accepted October 5, 1992

Abstract. — The emission of hydrogen lines and continua from solar prominences is investigated using a set of 140 simple models, covering the range of physical conditions usually assumed for these objects. These models are plane-parallel, isobaric and isothermal. The computations have been carried out using a 20 level plus continuum hydrogen atom, and taking into account the effects of partial frequency redistribution in the Lyman-α and β lines. The aim of these computations is twofold: Firstly, to describe the variations of hydrogen lines and continua emitted by prominences when physical conditions vary. Secondly, to provide observers with some diagnostic tool to interpret data such as intensity ratios, line widths, etc... The results of computations are given as mixed table-figure panels, each of them corresponding to a given model and summarizing the associated physical parameters and the principal features of the emitted hydrogen spectrum. Finally, for some specific parameters (or couple of parameters), we present figures illustrating the variations of these quantities across the whole set of models.

Key words: sun: prominences — line: formation — radiative transfer

1. Introduction

The importance of prominences in solar and plasma physics is evidenced by a number of recent papers devoted to their formation, their stability, the conditions for their eruption and also to their physical conditions (see e.g. the proceedings of the Hvar Colloquium edited by Ruždjak & Tandberg-Hanssen, 1990, and Priest's book, 1989). Actually, in spite of many progresses made both observationally and theoretically, the diagnostic of these structures is still uncertain. This is true for the dynamics in prominences, which is basic for understanding the material exchange between the prominence and the surrounding corona and chromosphere. This is also true for the diagnostic of important parameters such as temperature, density, ionization degree, which are also critical for any realistic MHD modeling of prominences. After it had been realized that prominences were definitely out of local thermodynamic equilibrium (Hirayama 1963), much work had been performed in the computation of excitation and ionization within these structures, the most important one starting with the study of Heasley et al. (1974) who adapted the NLTE linearization code to the problem of illuminated slabs. The road was open to systematic and accurate modeling of one dimensional structures irradiated from the sides. The next papers by Heasley & Mihalas (1976) (HM1) and Heasley & Milkey (1976) (HM2) were devoted to the computation of a series of hydrogen and helium lines and continua intensities emitted by a set of slabs with varying temperature, pressure, column mass, helium abundance, etc.. Sophisticated models in radiative balance or including an extra energy input or magnetic pressure were also built. These predictions were compared with the most recent measurements of absolute intensities performed with the Mees Observatory photoelectric device of Landman and co-workers (see e.g. Landman 1986, and references therein). More observations of different lines from different atoms were also performed by Stellmacher and collaborators (e.g. Stellmacher 1979; Stellmacher & Wiehr 1981). However, HM1 failed to predict the low Hβ observed intensity along with the observed ratios of hydrogen to helium lines. HM2 improved this situation with the use of thinner and slightly hotter models. However the predicted CaII K intensities were far larger than observed ones (Heasley et al. 1977). The authors wrote at that time that "a great deal of work on quiescent prominences remains to be done..", a situation that they contributed to change (Heasley & Milkey 1978, 1983) (HM3 and HM4). HM3 extended the computations to the Ca II lines: it was shown for instance that the ratio of CaII (8542 Å) to Hβ integrated intensities is sensitive to the pressure. The Balmer decrement was found to be controled by incident radiation in Balmer lines. HM4 was devoted to a thorough analysis of the Lyman

continuum: it was demonstrated that the color temperature of the Lyman continuum is a good indicator of the electron temperature. One can conclude from this basic work that such a grid of models provided a wide range of predictions concerning emissions in lines and continua and their correlations with physical parameters. At this time low pressure models ($p \approx 0.02$ dyn cm^{-2}) seemed to fit known observations and the temperature range was limited to 7500 K to 9000 K.

However, such a heavy modeling suffered some drawbacks. Firstly, the authors themselves (HM3) noted that "with regard to the model calculations, the most uncertain aspect is the accuracy to which we know the illuminating radiation incident on the prominences". This was especially true for uv lines and continua: for Lyman lines for instance, both intensities and profiles were poorly known. Secondly, it was established at that time that the nature of the frequency redistribution in the scattering process plays an important role, especially in line wings of chromospheric Lα and Ca II K (Milkey & Mihalas 1973; Shine et al. 1975). Actually, in prominences too, Milkey et al. (1979) found that the partial redistribution (PRD) led to Lα wings about one order of magnitude lower than wings formed in complete redistribution (CRD). With OSO-8 results (e.g. Vial et al. 1979 or Vial 1982), both chromospheric and prominence profiles were made available in Lα, Lβ of H I and also Mg II h and K lines, with the bonus of Ca II H and K lines that allowed to compare with previous ground-based observations (cf. the Lα Hα comparison by Heinzel & Vial 1983). It was then possible to implement realistic incident profiles in computations and also to compare computed profiles of resonance lines with observed ones. Heinzel et al. (1987) (hereafter Paper I) computed seven low pressure and low temperature models where PRD and OSO8 incident profiles were implemented. Such models provided a reasonable agreement with observations. Concerning the Lα profile, Paper I showed that both PRD and correct incident radiations were absolutely necessary to obtain a reasonable reproduction of the observed profiles. However, provided that these precise incident radiations were implemented, the resulting frequency-integrated intensities computed with PRD or CRD were about the same (the lower Lα integrated intensities in PRD found by Milkey et al., 1979, were actually an artefact of inadequate incident radiations). But the computations of Paper I were not able to reproduce the observed Lα to Lβ ratio. Heinzel et al. (1988) obtained some improvement concerning the Lβ profile and intensity by introducing a transition zone between the prominence and the coronal medium, but the Lβ Lα ratio was still too low to match the observations. In addition, the computations of Paper I were limited to a small variety of models and a small number of atomic levels (5 discrete levels plus one continuum), as compared to HM3 who used 35 levels!

So we think that it is now appropriate to construct a wider set of models with the latest improvements concerning incident radiation and atomic physics. Such a set and its predictions about observable quantities (especially line profiles) can help to identify the spectral features sensitive to a given physical parameter; it can help to understand the processes at work and it can provide a readily accessible diagnostic tool for a wide range of solar objects (quiescent and active prominences, cool coronal loops, etc..).

2. Numerical procedures

In order to determine the hydrogen spectrum emitted by a model prominence, we have to solve several equations governing the pressure equilibrium, ionization and statistical equilibrium of hydrogen atoms, and radiative transfer in all optically thick transitions (lines and bound-free continua). Similar computations have been described in Paper I. They were carried out with the Ondřejov code assuming a 5 level plus continuum hydrogen atom, and solving all equations by the linearization technique. In the present paper, we use a different (IAS) code which is based on the equivalent-two-level-atom technique, the solution of statistical equilibrium equations being achieved by iteration (cf. Gouttebroze 1980). Originally, this code was designed for the modeling of semi-infinite atmospheres in hydrostatic equilibrium (Gouttebroze et al. 1978). Later on, it was modified to treat plane-parallel finite slabs with incident radiation on one side or two (Gouttebroze et al. 1986, Tsiropoula et al. 1986). Some improvements (such as the possibility of using an arbitrary number of atomic levels and transitions) have been added to obtain the present code. Radiative transfer equations, with partial frequency redistribution in Lyman lines, are solved by the Feautrier method, with variable Eddington factors (Auer & Mihalas 1970). We took advantage of the existence of these two independently developed codes to perform comparative computations, in order to detect eventual errors: we used exactly the same input data, atomic structure and prominence model, and obtained almost the same results concerning hydrogen excitation and ionization, and output radiation fields. Small discrepancies (up to 5 %) were found, which are probably due to the quite different structures of the codes and other details in numerical approaches. During these comparisons, it was found that the results were rather sensitive to frequency and depth discretizations, especially for PRD where both are strongly interrelated. In particular, it appeared necessary to use a broad frequency mesh (100 Doppler widths or so) for the Lyman lines.

2.1. Prominence models

Due to the necessity of limiting the number of free parameters, we use isothermal and isobaric slabs standing vertically above the solar surface. The emergent intensities are computed in the direction perpendicular to the slab. Each model is defined by its kinetic temperature, gas pressure and geometrical thickness. We use 7 values of gas pressure: 0.01, 0.02, 0.05, 0.1, 0.2, 0.5 and 1 dyn cm^{-2}, and 6 geometrical thicknesses: 200, 500, 1000, 2000, 5000 and 10000 km. For the temperatures, there are 3 principal values: 6000, 8000 and 10000 K, for which we compute all the combinations of the preceding parameters, i.e. 3*5*6 = 126 models. We also explore two "extreme" temperatures: 4300 and 15000 K, but restricting in this case our investigation to a thickness of 5000 km, which gives 2*7 = 14 additional models. The microturbulent velocity, which appears to have secondary importance in the case of hydrogen lines, is fixed arbitrary to 5 km/s.

2.2. The model hydrogen atom

In the case of the hydrogen atom, the proper number of levels to be used in computations is rather arbitrary. The precision, but also the necessary computer time, increase with the number of levels. In order to estimate the errors, we have performed a series of computations concerning the same prominence model ($T = 8000$ K, $P = 0.1$ dyn cm^{-2}, $\Delta z = 2000$ km) with different numbers of levels ranging from 5 to 30 discrete levels plus continuum. These results are displayed in Table 1. The test on the LTE departure coefficients $[b_j = (n_j/n_\infty) / (n_j/n_\infty)_{LTE}]$ for level populations is based on the fact that these coefficients should tend to unity when the index $[j]$ of the level increases. This condition is satisfied within 26 % for 10 levels, 8 % for 15, 2 % for 20 and less than 1 % for 30. Concerning the computation of emergent intensities, the consequences of the limitation of the number of energy levels are variable according to the location of the transition in the energy diagram. For instance, for Lα, the correct intensity is reached with 5 levels plus continuum only, while the same model atom, Hγ is 35 % too low. In general, for the transitions treated in this paper, the differences between intensities obtained with 20 and 30 discrete levels lie within 1 %.

We concluded, on the basis of this test, that a 20 level plus continuum hydrogen atom gives a precision sufficient for our purpose and decided to use it throughout our set of computations.

Concerning atomic parameters, we use the formulae by Johnson (1972) to compute oscillator strengths and transition rates for excitation and ionization by collisions. We did not go into details of PRD since also other model characteristics (geometry, isobaric-isothermal structure, etc.) are oversimplified. Therefore we use here the same approach as in Paper I, i.e. the "standard" PRD instead of considering much more complicated PRD-interlocking effects (Cooper et al. 1990).

Table 1. Results of computation for the same prominence model ($T = 8000$ K, $p = 0.1$ dyn cm^{-2}, $\Delta z = 2000$ km) but different approximations for the hydrogen atom. Each column corresponds to a model atom, which includes a number of discrete levels (indicated in the first row) and one continuum. b_j is the LTE departure coefficient for level (j). E represents the energy (intensity integrated over frequency) for the line indicated into parentheses. The number which follows immediately indicates the power of ten by which the numbers in the columns should be multiplied to obtain the energy in cgs units. Last row: I_0 (L.C.) is the intensity at the head of the Lyman Continuum (same conventions)

Number of discrete levels		5	10	15	20	25	30
b_1		213.	221.	207.	201.	199.	199.
b_2		58.8	60.9	57.1	55.6	55.1	55.0
b_3		2.26	2.50	2.35	2.29	2.27	2.27
b_4		0.96	1.19	1.13	1.11	1.10	1.10
b_5		0.77	1.18	1.12	1.10	1.09	1.09
b_6			1.55	1.47	1.43	1.42	1.42
b_7			1.43	1.34	1.30	1.29	1.29
b_8			1.33	1.23	1.19	1.18	1.18
b_9			1.28	1.16	1.12	1.11	1.11
b_{10}			1.26	1.12	1.08	1.06	1.06
b_{11}				1.10	1.05	1.04	1.04
b_{12}				1.09	1.04	1.03	1.02
b_{13}				1.08	1.03	1.02	1.02
b_{14}				1.08	1.03	1.01	1.01
b_{15}				1.08	1.02	1.01	1.01
b_{16}					1.02	1.01	1.01
b_{17}					1.02	1.01	1.01
b_{18}					1.02	1.01	1.00
b_{19}					1.02	1.01	1.00
b_{20}					1.02	1.01	1.00
b_{21}						1.01	1.00
b_{22}						1.01	1.00
b_{23}						1.01	1.00
b_{24}						1.01	1.00
b_{25}						1.01	1.00
b_{26}							1.00
b_{27}							1.00
b_{28}							1.00
b_{29}							1.00
b_{30}							1.00
E(Lα)	(+4)	2.83	2.84	2.82	2.82	2.81	2.81
E(Lβ)	(+1)	7.99	8.25	8.21	8.19	8.19	8.19
E(Hα)	(+5)	1.00	1.08	1.07	1.06	1.06	1.06
E(Hβ)	(+4)	1.07	1.30	1.28	1.28	1.27	1.27
E(Hγ)	(+3)	3.01	4.52	4.48	4.45	4.45	4.45
E(Hδ)	(+3)		2.79	2.74	2.71	2.71	2.71
E(Hϵ)	(+3)		1.42	1.38	1.36	1.36	1.36
E(Pα)	(+3)	3.11	3.79	3.75	3.72	3.71	3.71
I_0(L.C.)	(-12)	5.59	5.37	5.65	5.78	5.82	5.83

2.3. Incident intensities

In Paper I, we showed that the definition of the intensities impinging on the prominence at wavelengths close to the principal transitions of hydrogen (especially Lyman and Balmer lines) had a major importance for the statisti-

cal equilibrium of level populations and the computation of outgoing intensities. So that, before undertaking the present computations, we have tried to establish these incoming line profiles and other intensities as carefully as possible.

For all models, we assume a mean altitude of 10000 km above the solar surface. In the absence of limb-darkening, the incoming intensities on each side of the slab are equal to the intensity emitted by the sun multiplied by a dilution factor of 0.416. For Lα and Lβ, where limb-darkening is negligible, we use the intensities averaged on the disk measured by OSO-8, and multiply them by this dilution factor. For Lγ and Lδ, the detailed profiles are not known but the total intensity (integrated over frequency) has been measured by Vernazza & Reeves (1978). For these two lines, we assume profiles identical to that of Lβ, but multiply the intensity by scaling factors of 0.230 and 0.112 for Lγ and Lδ, respectively.

In the case of Balmer, Paschen and Brackett lines, limb darkening is no more negligible so that, instead of using dilution factors, we integrate numerically the intensities over the solid angle centered on the prominence and tangent to the solar sphere, with the appropriate darkening for each ray. We use the data as described in Paper I and obtain detailed incoming intensities for the 10 lines whose upper level is lower or equal to 5. These intensities are represented in Fig. 1.

The lines whose upper level goes from 6 to 20 are less important for statistical equilibrium, so that we adopted the following simplified treatment. The Lyman lines were set into detailed balance, while the lines of the other series were treated as optically thin (which is true for all the models under consideration), and the intensities were assumed equal to those of the continuum at the same frequencies.

For these subordinate lines as well as for the continua, it was found convenient to use a table of mean brightness temperatures for the solar disk, as a function of wavelength. This relation, established from Makarova & Kharitonov (1969, 1972), Allen (1973) and the OSO-6 measurements for the Lyman continuum (see Heasley et al. 1974), is given in Table 2. For each bound-free continuum, we define a set of 10 frequencies, interpolate in the table to get the mean brightness temperatures corresponding to these frequencies, convert them into intensities and multiply by the dilution factor (0.416).

For all transitions, lines or continua, we first estimate the optical thickness of the slab (at the frequency of maximum opacity) in order to decide about the appropriate treatment of the transition. If the optical thickness is lower than 0.1, the intensity is assumed constant throughout the slab (optically thin approximation); otherwise, we solve the radiative transfer equation by the Feautrier method. In general, the Lyman lines and continuum were found to be optically thick (except for the lowest values of pressure and thickness), while the first two Balmer lines were sometimes thick and sometimes thin, according to the model. Other transitions were practically always optically thin.

Table 2. Brightness temperature (T_B) of the average solar disk as a function of wavelength (λ)

λ (μm)	T_B (K)	λ (μm)	T_B (K)	λ (μm)	T_B (K)
.0114	23480	.15	4761	1.0	5786
.0137	22560	.18	4884	1.2	5880
.0171	21160	.20	4965	1.4	6049
.0195	20240	.22	5201	1.6	6302
.0228	18920	.24	4978	1.8	6286
.0279	16920	.26	5116	2.0	6072
.0359	13500	.28	5207	3.0	5730
.0419	11700	.30	5483	4.0	5500
.0504	9600	.35	5604	5.0	5450
.0592	8500	.40	5694	10	5050
.0718	7200	.50	5906	20	4740
.0803	6700	.60	5845	50	4500
.0911	6500	.70	5850	100	4370
.0912	5000	.80	5792	200	4400
.12	5200	.90	5729	300	4550

3. Detailed results

The results of these computations are displayed in form of a series of 44 panels, each of them being dedicated to one prominence model. In order to save space, we do not give these detailed results for all the 140 models defined in Sect. 2.1, but for a subset of 44 ones, which corresponds to 4 pressures (0.01, 0.05, 0.2 and 1 dyn cm^{-2}) and 3 thicknesses (200, 1000 and 5000 km). However, the full set of models will be used in Figs. 2, 3 and 4, which are described in the following section. Each panel contains 3 rows of general parameters, one table and 9 plots.

The first row indicates the 4 quantities that define the model: temperature T in kelvins, gas pressure P in dyn cm^{-2} (turbulent, magnetic and radiation pressure are not included), transversal thickness Δz in km, and microturbulent velocity v_T in km s^{-1}.

The second and third rows contain quantities provided by the computations:

- the column mass m in g cm^{-2}.
- the maximum S^{23}_{max} of the line source function for Hα. This quantity is used to scale the last plot of the panel. It is expressed in erg s^{-1} cm^{-2} sr^{-1} Hz^{-1}.
- the total hydrogen number densities n_H(c) and n_H(s), in the center and at the surface of the slab, respectively, in cm^{-3}.
- the optical thickness τ(L.c.) of the slab at the head of the Lyman continuum.
- the same for τ(B.c.) at the head of the Balmer continuum.
- the electron densities n_e(c) and n_e(s), in the center and at the surface of the slab, respectively, in cm^{-3}.

These three rows are followed by a table which gives the main properties of hydrogen lines: the lines are identified by columns 1 and 2 which indicate their lower and upper level, respectively. Other columns give:
3: (τ) optical depth of the slab at line center.
4: ($I_{\max}$) maximum intensity of the profile in cgs units (erg s^{-1} cm^{-2} sr^{-1} Hz^{-1}); this quantity may be used to scale the profiles represented in the 6 first plots below.

5: ($E_{\rm tot}$) this "total energy" is the intensity integrated over frequency in cgs units (erg s^{-1} cm^{-2} sr^{-1}).

6: (FWHM) full width at half maximum of the line, in Å.

For this table, we have chosen the first three lines of the Lyman series, the first two of the Balmer series and the first Paschen line. Since the Balmer series is the most often observed, we have added 3 extra Balmer lines.

Under this table, there are 9 plots showing line profiles and other parameters. Plots 1 to 6 represent the profiles of the 6 first lines of the above table, namely Lα, Lβ, Lγ, Hα, Hβ, and Pα. The abscissae are the wavelengths (relative to line center) in Å. The ordinates are normalized to 1: to obtain the absolute intensity, it is necessary to multiply by the corresponding $I_{\max}$ value from the table. The profiles of Hγ, Hδ and Hε are not given: since these lines are almost always optically thin, they have quasi-gaussian profiles that may be easily recovered knowing $I_{\max}$ and FWHM.

The plots of the lowest row represent:

– Plot 7: Variation of electron density across the half of the slab (which is symmetrical). Abscissae are undimensioned: 0 represents the surface and 1 the middle of the slab. The unit for electron density is 10^{10} cm^{-3}.

– Plot 8: decimal logarithm of the intensity in the Lyman continuum versus relative frequency (ν/ν_0). The intensity is expressed in cgs units (erg s^{-1} cm^{-2} sr^{-1} Hz^{-1}). ν_0 is the frequency of the head of the Lyman continuum.

– Plot 9: variation of the Hα source function across the half slab. Abscissae are the same as in Plot 7. The intensity is normalized to the maximum value $S^{23}_{\max}$ given in the second row of the panel. This last plot is often surprising, since the relative source function does not seem to reach its maximum value of 1. This effect is due to a very sharp rise of the source function that often occurs in the outermost layers of the slab. The region where this rise takes place is so thin that it is negligible for the computation of Hα intensities.

4. Recapitulation and conclusion

To illustrate the possible use of the above prominence catalog, we can now display some comparative diagrams including the whole set of models. We can for instance study the relation between the energy emitted in one hydrogen line and a physical parameter, or another line or continuum. Among the most often measured quantities concerning the prominences, are the total energies emitted in the principal lines of the Balmer series. Figure 2a represents the variation of energy in Hα as a function of that in Hβ. This relation is practically linear at small optical depths. At higher depths, there appears certain divergence, principally related to the temperature: hot structures appear to have a (Hα /Hβ) ratio higher than cool ones. If one wants to compare these computations with observations, one has to take into account the filling factor arising from the fact that the slit of the spectrograph is generally not entirely filled by the prominence. In order to simulate this effect, for filling factors in the range [0.1, 1], we take each point of the preceding diagram, and multiply both coordinates successively by 0.1, 0.2, 0.3, ..., 0.9 and 1. We thus obtain a cloud of points, 10 times more dense than the initial one, which is represented in Fig. 2b. Comparison with available observations (see, e.g., Stellmacher 1979) shows that practically all observed points lie within the area defined by this cloud.

Among different correlations concerning the Balmer lines, we have found a rather good one between the total energy in Hα and the so-called "emission measure" $M_{\rm E} = \int n_{\rm e}^2 {\rm d}z$. This effect is illustrated in Fig. 3.

Concerning the Lyman continuum, we have two remarks to do. If we plot the intensity at the head of the Lyman continuum as a function of the column mass (Fig. 4a), we can see that, except for very thin structures, the intensity is remarkably constant at low temperatures (4300 and 6000 K). It is still slowly varying at 8000 K. On the contrary, the intensity grows rapidly with pressure for higher temperatures (10000 and 15000 K). The other remark concerns the slope of the Lyman continuum. A simple examination of the preceding panels shows that this slope depends essentially on temperature. Using the two first points of the frequency mesh, we can compute an approximate value for (d ln I/d ln ν) close to the head of the continuum, and convert it into a "color temperature". The result is shown in Fig. 4b. It appears that, except for very thin structures, the color temperature remains close to the electron temperature. This is in agreement with similar findings by Heasley & Milkey (1983), which confirms the possibility of using the Lyman continuum slope as a temperature indicator.

The present set of models does not pretend to be a realistic representation of actual prominences: it is known that these objects have complicated shapes, inhomogeneous structures, and are surrounded by transition zones with steep temperature gradients (cf., e.g., Heinzel & Vial 1992). However, it is easy to see that a systematic modeling of inhomogeneous prominences would require a number of models too large to be tractable from the computational point of view. So that, the ambition of the present work is simply to give some general and approxi-

mate relations between physical conditions in prominences and observations of the hydrogen spectrum. It could also serve as a benchmark for testing other similar codes or developing more sophisticated ones.

Concerning the field of space instrumentation, we may note that the Lyman lines, as well as the Lyman continuum, will be detectable by the SOHO/SUMER experiment, so that computations similar to those reported here will be useful for the interpretation of these future observations.

In this last section, we have not exhausted the conclusions that could be drawn from the computations. We plan to present a more detailed analysis of these results in a subsequent paper.

Acknowledgements. We are indebted to T. Hirayama for encouraging us to undertake the computations of such a grid of models. The main part of numerical computations was performed on the Cray-2 computer of the "Centre de Calcul Vectoriel pour la recherche" with computing time allocated by the "Centre national d'Etudes Spatiales".

References

Allen C.W. 1973, "Astrophysical Quantities" (3rd edition)., The Athlone Press, London
Auer L.H., Mihalas D. 1970, MNRAS 149, 65
Cooper J., Ballagh R.J. and Hubeny I. 1990, ApJ 344, 949
Gouttebroze P. 1980, "Formation des raies spectrales et oscillations dans la chromosphère solaire", Ph.D. Thesis (Paris)
Gouttebroze P., Lemaire P., Vial J.C., Artzner G. 1978, ApJ 225, 655
Gouttebroze P., Vial J.C., Tsiropoula G. 1986, A&A 154, 154
Heasley J.N. and Mihalas D. 1976, ApJ 205, 273 (HM1)
Heasley J.N., Mihalas D. and Poland A.P. 1974, ApJ 192, 181
Heasley J.N. and Milkey R.W. 1976, ApJ 210, 827 (HM2)
Heasley J.N. and Milkey R.W. 1978, ApJ 221, 677 (HM3)
Heasley J.N. and Milkey R.W. 1983, ApJ 268, 398 (HM4)
Heasley J.N., Milkey R.W. and Engvold O. 1977, Solar Phys. 51, 315
Heinzel P., Gouttebroze P. and Vial J.-C. 1987, A&A 183, 351 (Paper I)
Heinzel P., Gouttebroze P. and Vial J.-C. 1988, in "Workshop on Dynamics and Structure of Solar Prominences", eds. E. Priest and J.L. Ballester, Mallorca, p. 71
Heinzel P., Vial J.-C. 1983, A&A 121, 155
Heinzel P., Vial J.-C. 1992, in "Solar Physics and Astrophysics at Interferometric Resolution", eds. L. Damé and T.D. Guyenne, ESA SP-344, Paris, p. 57
Hirayama T. 1963, PASJ 15, 122
Johnson L.C. 1972, ApJ 174, 227
Landman D.A. 1986, ApJ 305, 546
Makarova E.A., Kharitonov A.V. 1969, SvA, 12, 599
Makarova E.A., Kharitonov A.V. 1972, "Distribution of Energy in the Solar Spectrum and the Solar Constant", Nauka Publishing House, Moscow (English translation: NASA TTF-803)
Milkey R.W. and Mihalas D. 1973, ApJ 185, 709
Milkey R.W., Heasley J.N., Schmahl E.J. and Engvold O. 1979, in "Physics of Solar Prominences", IAU Colloq. 44, eds. E. Jensen, P. Maltby and F.Q. Orrall, P. 53
Priest E.R. (ed.) 1989, "Dynamics and Structure of Quiescent Solar Prominences", Kluwer Academic Publishers, Dordrecht
Ruždjak V. and Tandberg-Hansseen E. (eds.) 1990, IAU Colloq. No. 117, "Dynamics of Quiescent Prominences", Lecture notes in Physics 363, Berlin: Springer-Verlag.
Shine R., Milkey R.W. and Mihalas D. 1975, ApJ 199, 724
Stellmacher G. 1979, Solar Phys. 61, 61
Stellmacher G. and Wiehr E. 1981, Solar Phys., 71, 299
Tsiropoula G., Alissandrakis C., Bonnet R.M., Gouttebroze P. 1986, A&A 167, 351
Vernazza J.E., Reeves E.M. 1978, ApJS 37, 485
Vial J.-C., Gouttebroze P., Artzner G. and Lemaire P. 1979, Solar Phys. 61, 39
Vial J.-C. 1982, ApJ 253, 330

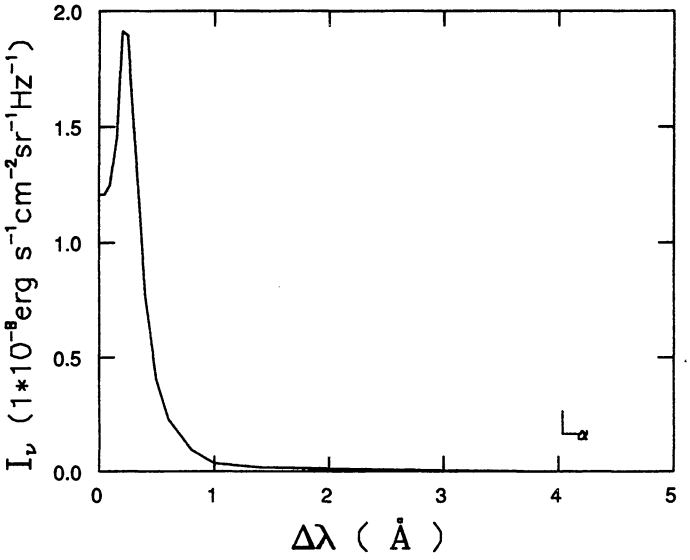

Fig. 1a.

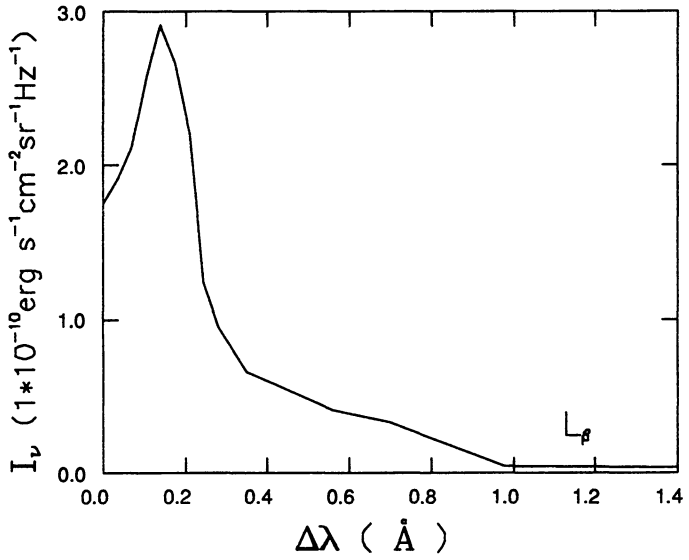

Fig. 1b.

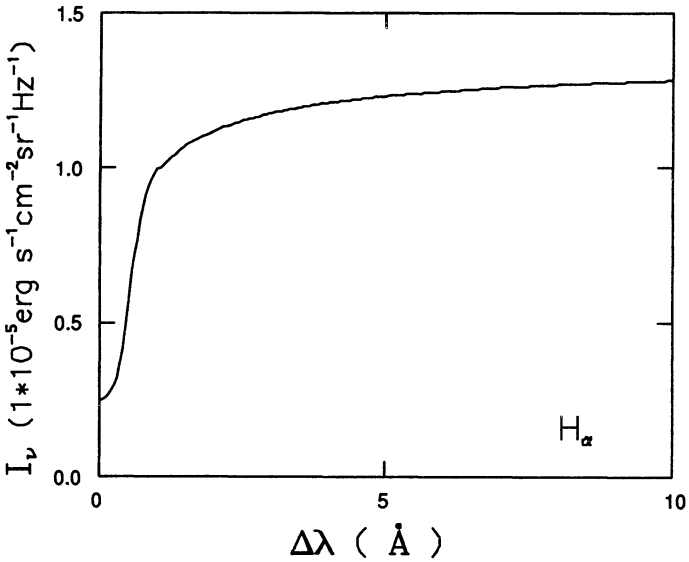

Fig. 1c.

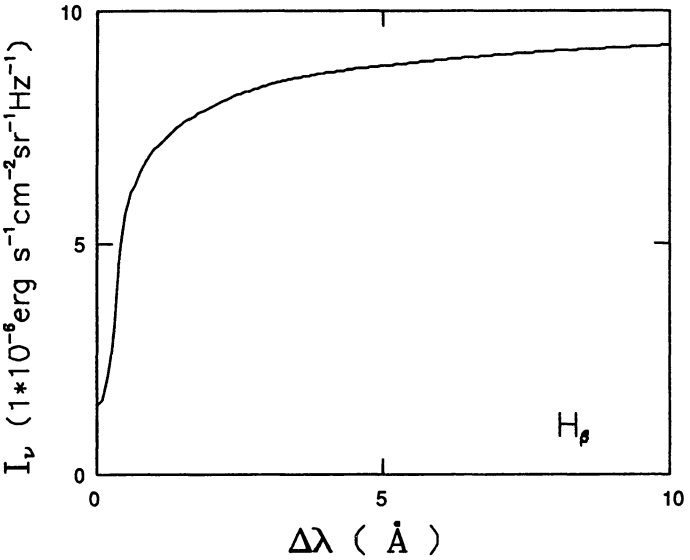

Fig. 1d.

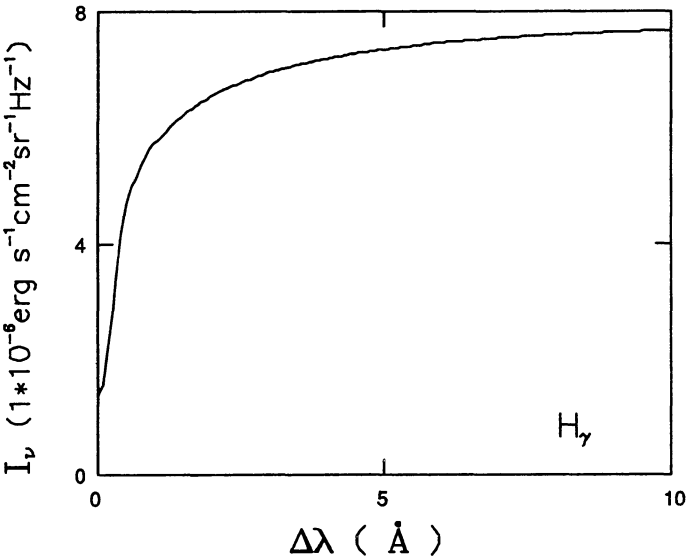

Fig. 1e.

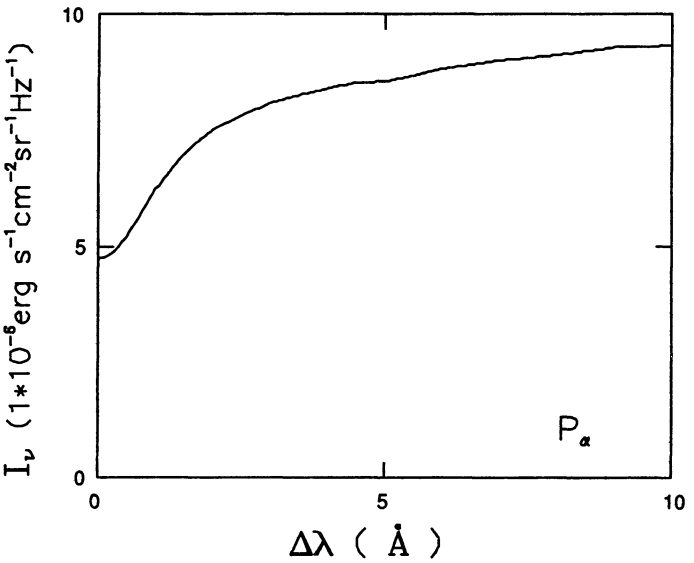

Fig. 1f.

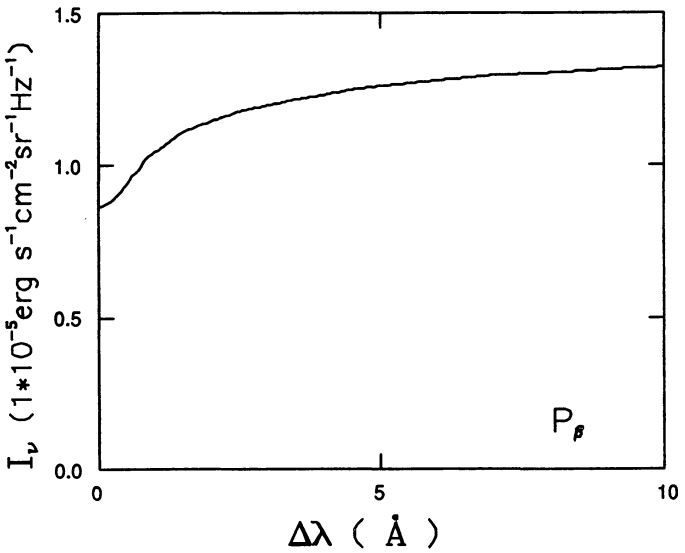

Fig. 1g.

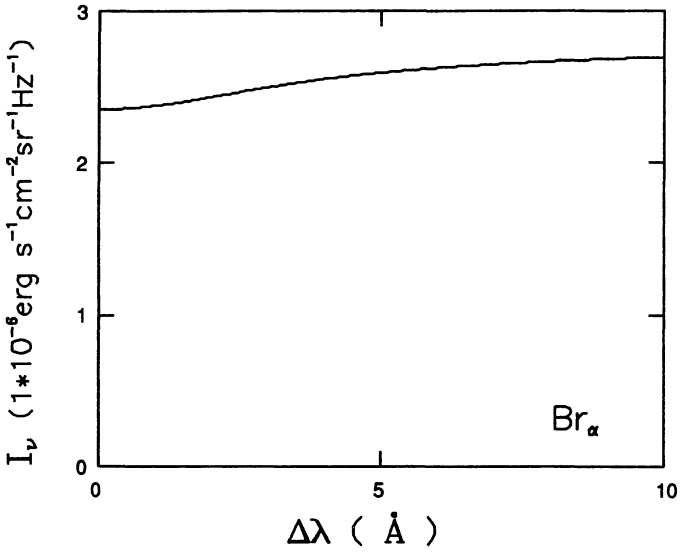

Fig. 1h.

Fig. 1. Incident intensities (with dilution factors included) for the principal hydrogen lines. a) Lα; b) Lβ; c) Hα; d) Hβ; e) Hγ; f) Pα; g) Pβ; h) Brα.

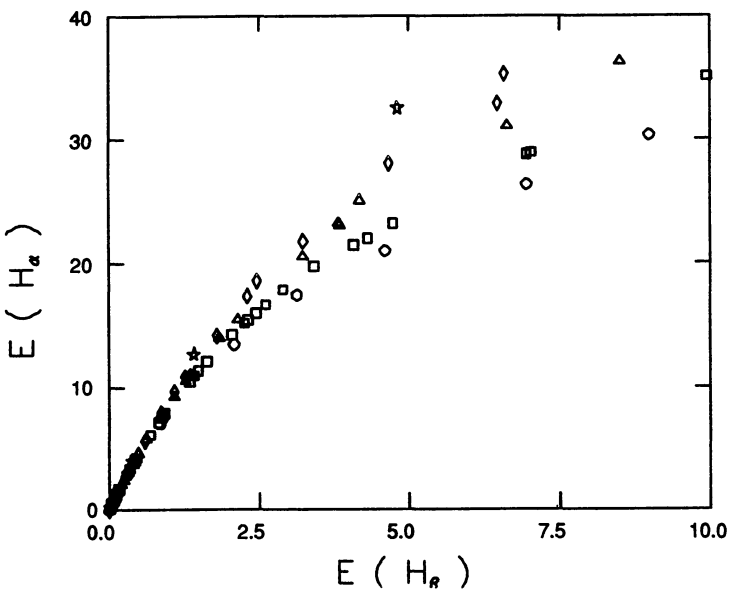

Fig. 2a.

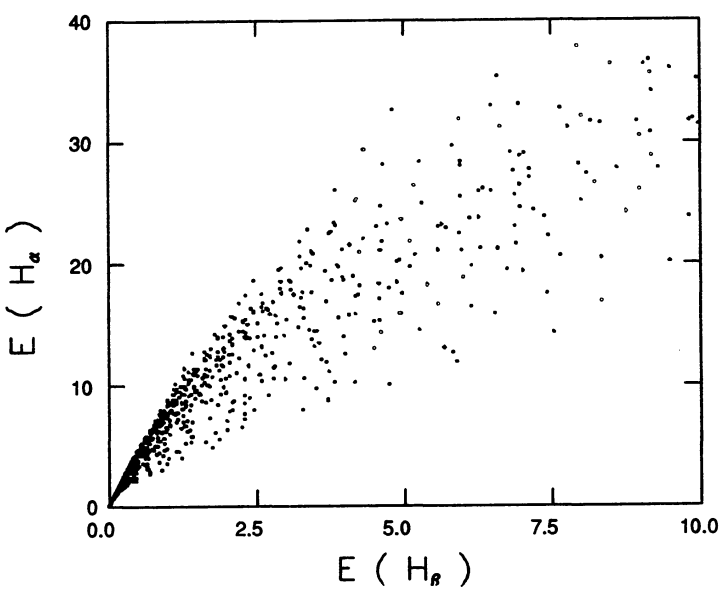

Fig. 2b.

Fig. 2. Total energy emitted in the Hα line as a function of that emitted in Hβ. Units are in 10^4 erg s^{-1} cm^{-2} sr^{-1}. a) direct results from computations; different symbols refer to different temperatures: circles: 4300 K, squares: 6000 K, triangles: 8000 K, losanges: 10000 K, stars: 15000 K. b) same results after multiplication by filling factors ranging from 0.1 to 1 (without indication of temperature)

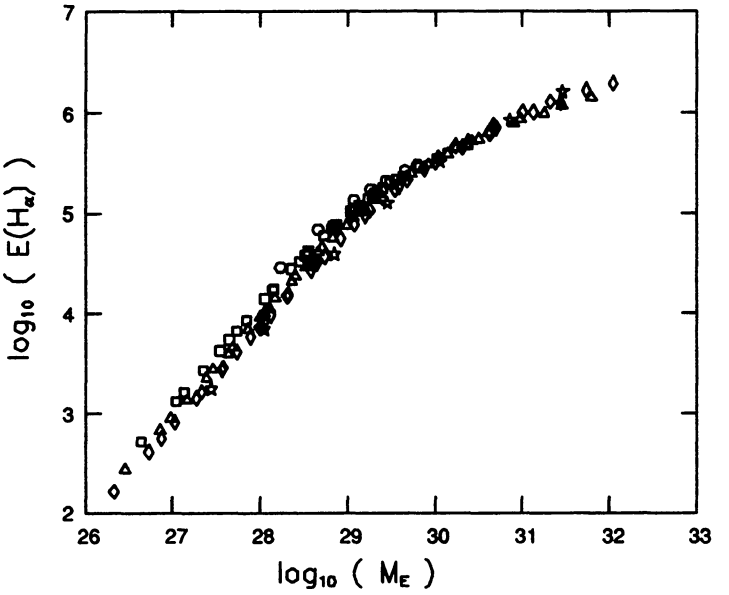

Fig. 3. Total energy emitted in the Hα line as a function of the emission measure $M_E = \int n_e^2 dz$. The scales are logarithmic and the two quantities are expressed in cgs units. Symbols refer to the same temperatures as in Fig. 2a

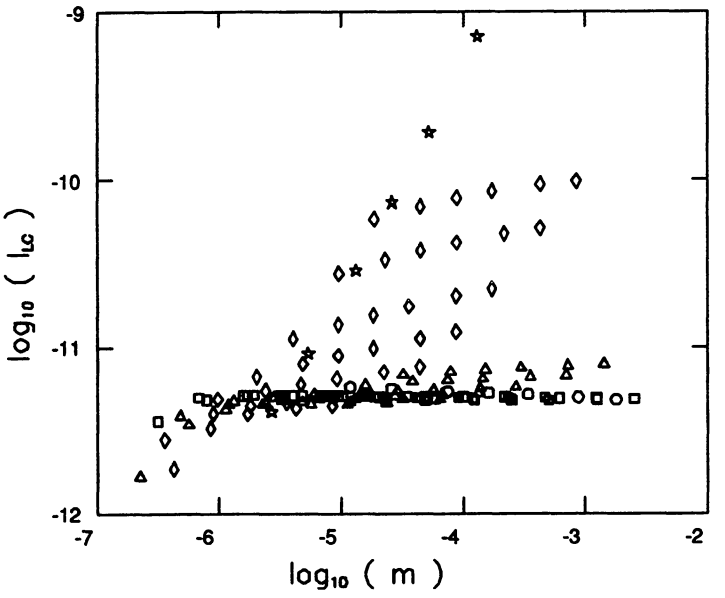

Fig. 4a.

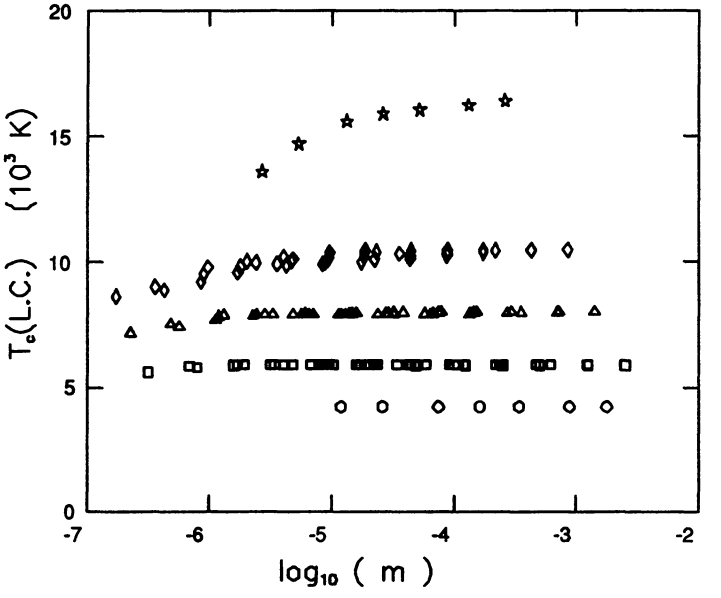

Fig. 4b.

Fig. 4. Properties of emissions in the Lyman continuum, as a function of the transversal column mass of the slab (cgs units), a) intensity at the head of the continuum. b) color temperature near the head. Symbols refer to the same temperatures as in Fig. 2a

T = 4300 P = 0.01 Δz = 5000 v_T = 5
m = 1.188E-05 S^{23}_{max} = 5.2E-06 n_H (c) = 1.0E+10 n_H (s) = 1.0E+10
τ(L.c.) = 1.31E+01 τ(B.c.) = 8.83E-06 n_e (c) = 5.9E+09 n_e (s) = 5.7E+09

hydrogen lines	LL	UL	τ	I_{max}	E_{tot}	FWHM
	1	2	1.60E+05	1.65E-08	1.95E+04	0.58
	1	3	2.57E+04	7.61E-11	4.79E+01	0.22
	1	4	8.92E+03	1.58E-11	9.05E+00	0.19
	2	3	4.06E-01	1.05E-06	2.96E+04	0.39
	2	4	5.62E-02	8.68E-08	3.15E+03	0.27
	3	4	6.11E-03	9.49E-08	8.85E+02	1.03
	2	5	1.88E-02	2.77E-08	1.12E+03	0.24
	2	6	8.79E-03	1.71E-08	7.36E+02	0.22
	2	7	4.89E-03	8.68E-09	3.88E+02	0.22

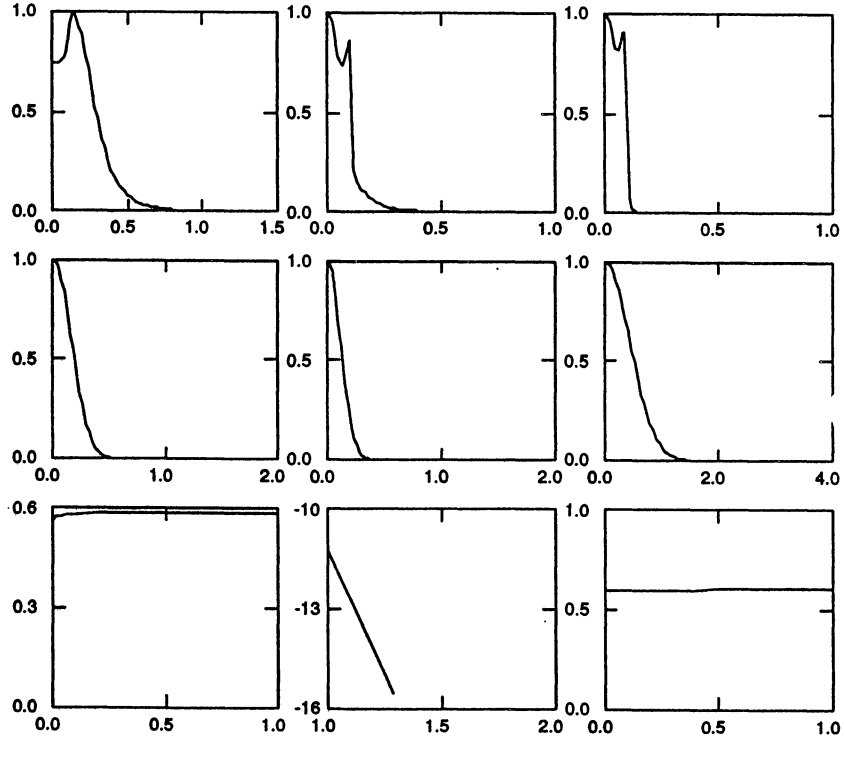

T = 4300 P = 0.05 Δz = 5000 v_T = 5
m = 7.440E-05 S^{23}_{max} = 5.4E-06 n_H (c) = 6.4E+10 n_H (s) = 6.1E+10
τ(L.c.) = 1.49E+02 τ(B.c.) = 6.23E-05 n_e (c) = 1.4E+10 n_e (s) = 1.8E+10

hydrogen lines	LL	UL	τ	I_{max}	E_{tot}	FWHM
	1	2	1.82E+06	1.50E-08	2.77E+04	0.86
	1	3	2.93E+05	8.20E-11	8.71E+01	0.35
	1	4	1.02E+05	1.61E-11	1.03E+01	0.21
	2	3	2.86E+00	3.62E-06	1.35E+05	0.53
	2	4	3.96E-01	5.48E-07	2.08E+04	0.29
	3	4	5.52E-02	6.89E-07	6.46E+03	1.04
	2	5	1.33E-01	1.92E-07	7.88E+03	0.24
	2	6	6.20E-02	1.20E-07	5.17E+03	0.23
	2	7	3.45E-02	6.15E-08	2.73E+03	0.22

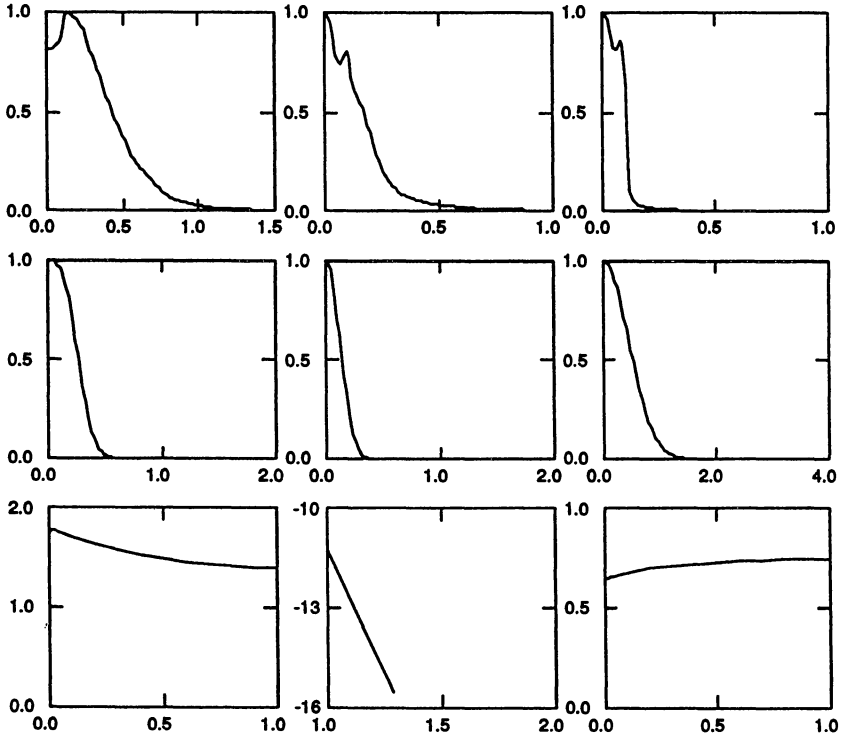

Fig. 5. Detailed results for 44 selected models (see Sect. 3)

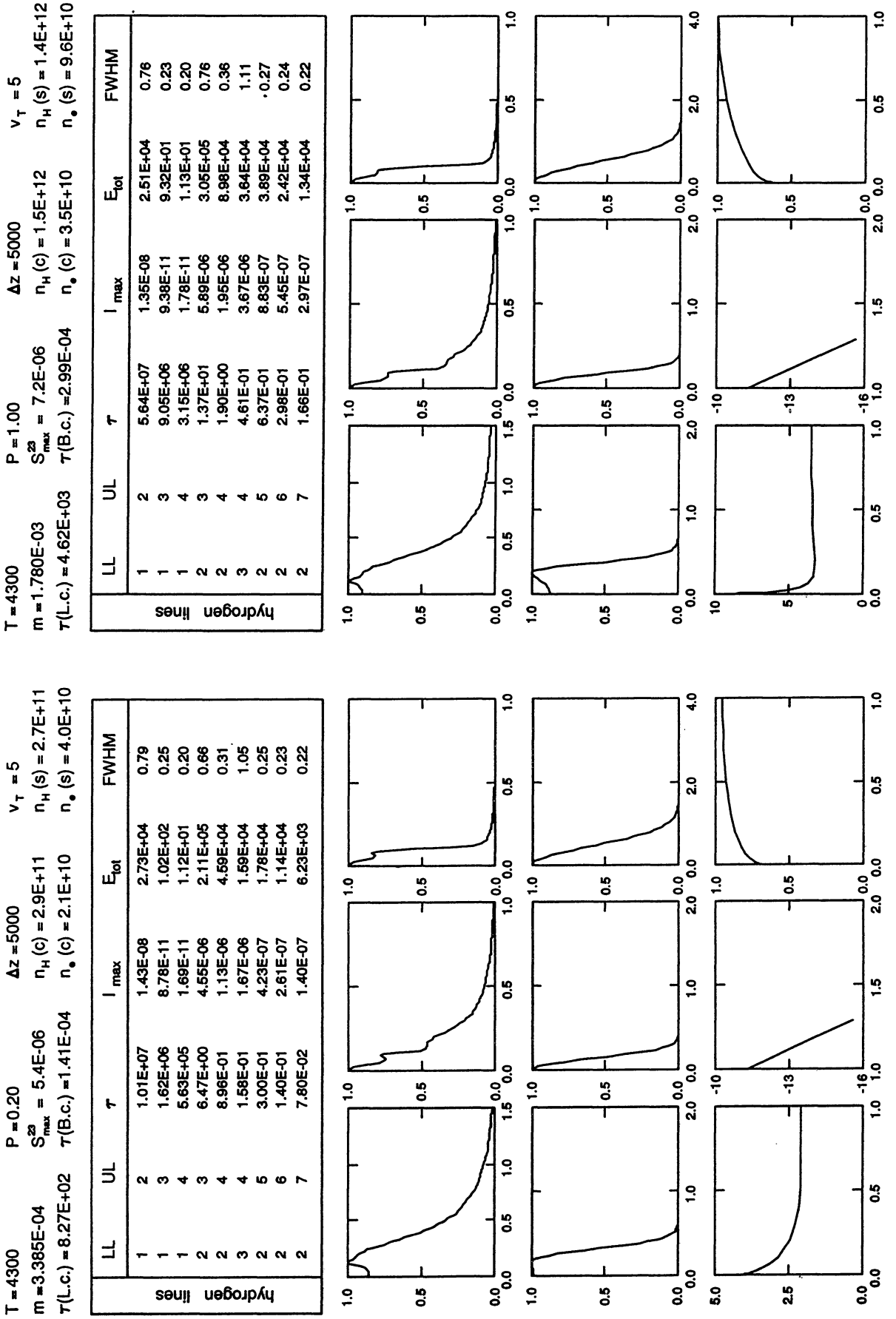

Fig. 5. continued

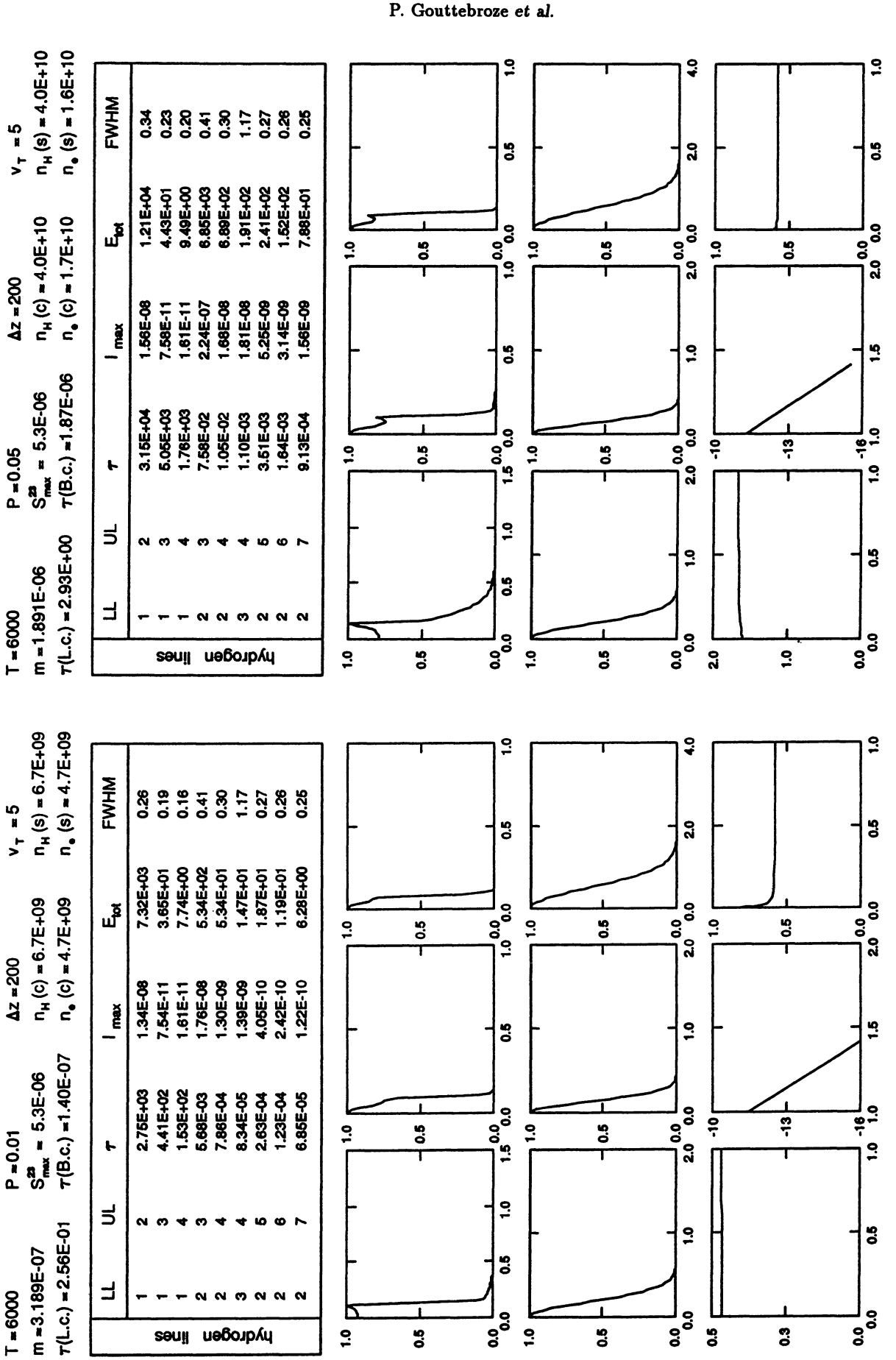

Fig. 5. continued

T = 6000 P = 0.20 Δz = 200 v_T = 5
m = 8.679E-06 S^{23}_{max} = 5.3E-06 n_H (c) = 1.8E+11 n_H (s) = 1.8E+11
τ(L.c.) = 1.79E+01 τ(B.c.) = 1.14E-05 n_e (c) = 4.0E+10 n_e (s) = 3.9E+10

hydrogen lines

LL	UL	τ	I_{max}	E_{tot}	FWHM
1	2	1.93E+05	1.60E-08	2.11E+04	0.64
1	3	3.09E+04	7.85E-11	5.66E+01	0.25
1	4	1.08E+04	1.62E-11	1.07E+01	0.22
2	3	4.61E-01	1.21E-06	3.89E+04	0.44
2	4	6.37E-02	1.00E-07	4.14E+03	0.31
3	4	7.22E-03	1.10E-07	1.17E+03	1.17
2	5	2.13E-02	3.18E-08	1.46E+03	0.27
2	6	9.96E-03	1.86E-08	9.00E+02	0.26
2	7	5.55E-03	9.20E-09	4.62E+02	0.25

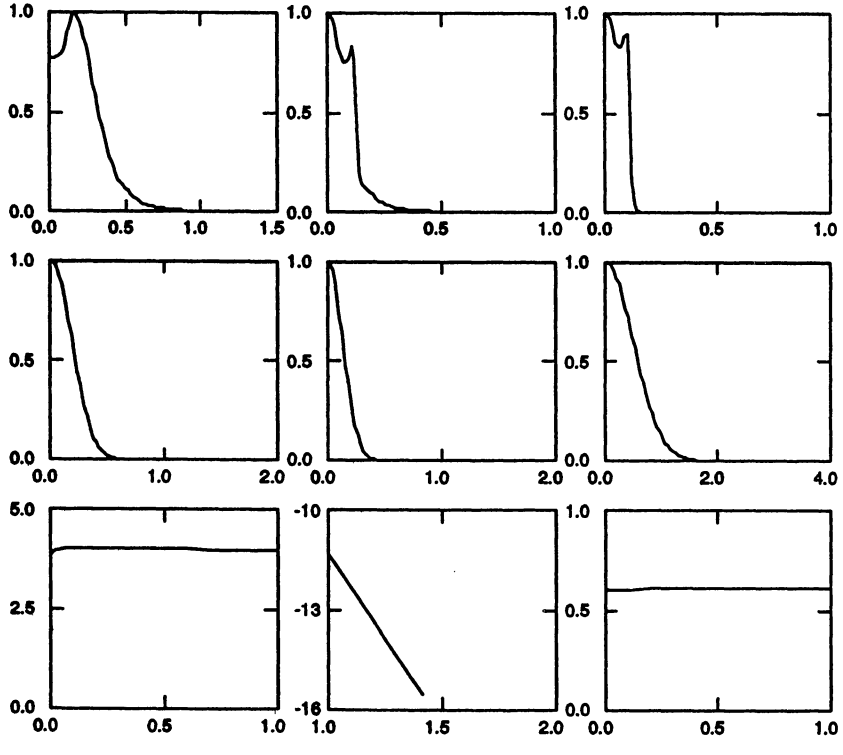

T = 6000 P = 1.00 Δz = 200 v_T = 5
m = 4.894E-05 S^{23}_{max} = 5.4E-06 n_H (c) = 1.0E+12 n_H (s) = 1.0E+12
τ(L.c.) = 1.21E+02 τ(B.c.) = 3.77E-05 n_e (c) = 6.4E+10 n_e (s) = 9.9E+10

hydrogen lines

LL	UL	τ	I_{max}	E_{tot}	FWHM
1	2	1.30E+06	1.39E-08	2.56E+04	0.85
1	3	2.08E+05	8.21E-11	8.20E+01	0.27
1	4	7.23E+04	1.63E-11	1.13E+01	0.23
2	3	1.53E+00	2.84E-06	1.05E+05	0.52
2	4	2.11E-01	3.19E-07	1.34E+04	0.31
3	4	2.72E-02	3.72E-07	3.95E+03	1.17
2	5	7.06E-02	1.05E-07	4.85E+03	0.27
2	6	3.30E-02	6.01E-08	2.92E+03	0.26
2	7	1.84E-02	3.00E-08	1.50E+03	0.25

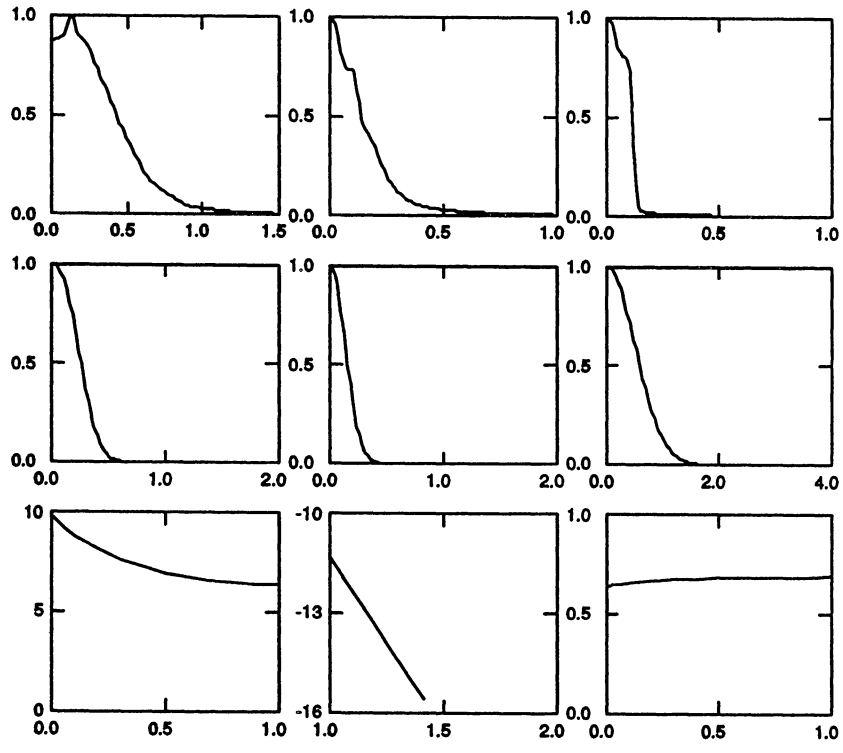

Fig. 5. continued

T = 6000 P = 0.01 Δz = 1000 v_T = 5
m = 1.587E-06 S^{23}_{max} = 5.3E-06 n_H (c) = 6.7E+09 n_H (s) = 6.7E+09
τ(L.c.) = 1.24E+00 τ(B.c.) = 7.45E-07 n_e (c) = 4.7E+09 n_e (s) = 4.7E+09

hydrogen lines	LL	UL	τ	I_{max}	E_{tot}	FWHM
	1	2	1.33E+04	1.44E-08	9.60E+03	0.30
	1	3	2.13E+03	7.56E-11	4.11E+01	0.21
	1	4	7.41E+02	1.61E-11	8.86E+00	0.19
	2	3	3.01E-02	9.12E-08	2.77E+03	0.41
	2	4	4.17E-03	6.76E-09	2.77E+02	0.30
	3	4	4.38E-04	7.23E-09	7.66E+01	1.17
	2	5	1.39E-03	2.10E-09	9.72E+01	0.27
	2	6	6.52E-04	1.27E-09	6.25E+01	0.26
	2	7	3.63E-04	6.35E-10	3.28E+01	0.25

T = 6000 P = 0.05 Δz = 1000 v_T = 5
m = 9.437E-06 S^{23}_{max} = 5.3E-06 n_H (c) = 4.0E+10 n_H (s) = 4.0E+10
τ(L.c.) = 1.46E+01 τ(B.c.) = 9.79E-06 n_e (c) = 1.7E+10 n_e (s) = 1.6E+10

hydrogen lines	LL	UL	τ	I_{max}	E_{tot}	FWHM
	1	2	1.56E+05	1.66E-08	2.01E+04	0.60
	1	3	2.51E+04	7.81E-11	5.50E+01	0.25
	1	4	8.72E+03	1.62E-11	1.06E+01	0.22
	2	3	3.96E-01	1.06E-06	3.39E+04	0.44
	2	4	5.48E-02	8.65E-08	3.56E+03	0.31
	3	4	6.15E-03	9.46E-08	1.00E+03	1.17
	2	5	1.83E-02	2.72E-08	1.25E+03	0.27
	2	6	8.57E-03	1.63E-08	7.91E+02	0.26
	2	7	4.77E-03	8.07E-09	4.07E+02	0.25

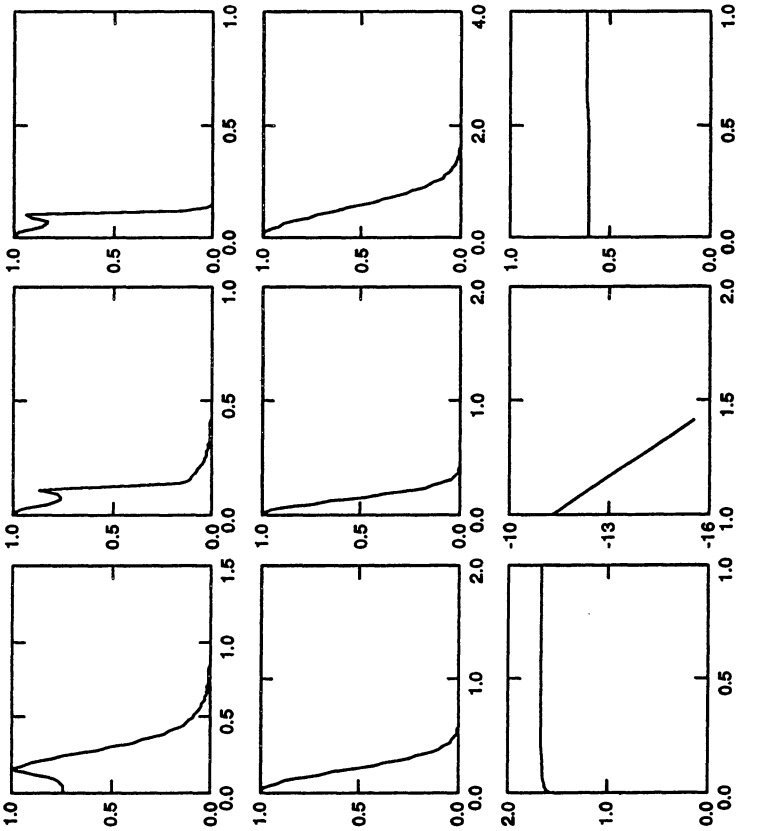

Fig. 5. continued

T = 6000 P = 0.20 Δz = 1000 v_T = 5
m = 4.461E-05 S^{23}_{max} = 5.4E-06 n_H (c) = 1.9E+11 n_H (s) = 1.8E+11
τ(L.c.) = 9.65E+01 τ(B.c.) = 4.24E-05 n_e (c) = 3.2E+10 n_e (s) = 3.9E+10

hydrogen lines	LL	UL	τ	I_{max}	E_{tot}	FWHM
	1	2	1.04E+06	1.48E-08	2.68E+04	0.86
	1	3	1.66E+05	8.21E-11	8.22E+01	0.29
	1	4	5.78E+04	1.63E-11	1.16E+01	0.23
	2	3	1.71E+00	3.01E-06	1.14E+05	0.53
	2	4	2.37E-01	3.53E-07	1.49E+04	0.32
	3	4	3.10E-02	4.17E-07	4.43E+03	1.17
	2	5	7.93E-02	1.17E-07	5.40E+03	0.27
	2	6	3.71E-02	6.91E-08	3.37E+03	0.26
	2	7	2.06E-02	3.44E-08	1.73E+03	0.25

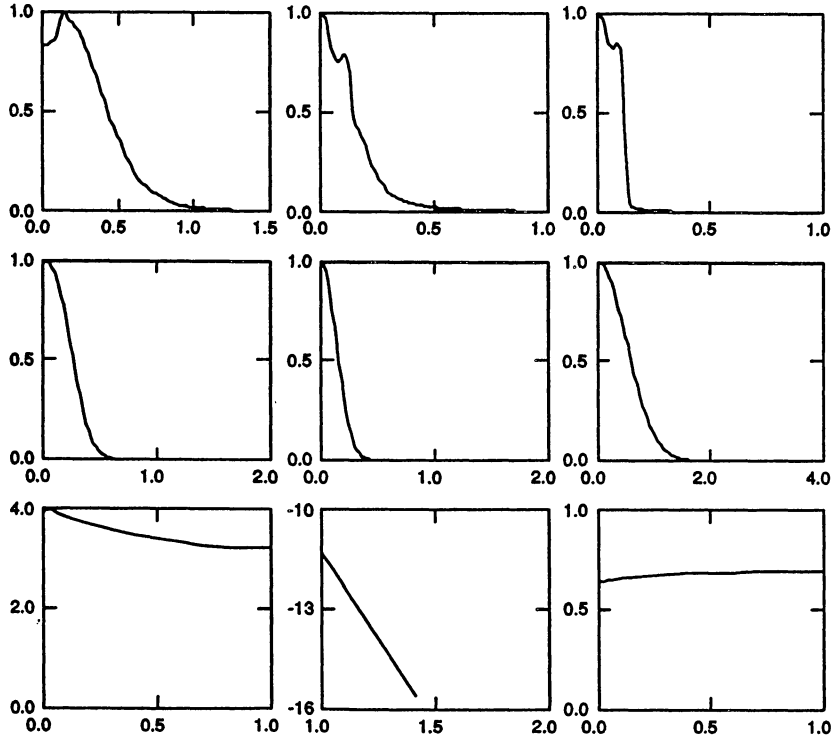

T = 6000 P = 1.00 Δz = 1000 v_T = 5
m = 2.500E-04 S^{23}_{max} = 5.4E-06 n_H (c) = 1.1E+12 n_H (s) = 1.0E+12
τ(L.c.) = 6.33E+02 τ(B.c.) = 8.48E-05 n_e (c) = 4.1E+10 n_e (s) = 1.0E+11

hydrogen lines	LL	UL	τ	I_{max}	E_{tot}	FWHM
	1	2	6.80E+06	1.39E-08	2.59E+04	0.77
	1	3	1.09E+06	8.70E-11	1.11E+02	0.26
	1	4	3.79E+05	1.66E-11	1.31E+01	0.22
	2	3	3.43E+00	4.03E-06	1.80E+05	0.63
	2	4	4.75E-01	6.65E-07	2.90E+04	0.33
	3	4	7.30E-02	8.55E-07	9.14E+03	1.18
	2	5	1.59E-01	2.33E-07	1.09E+04	0.28
	2	6	7.42E-02	1.37E-07	6.71E+03	0.26
	2	7	4.13E-02	6.87E-08	3.47E+03	0.25

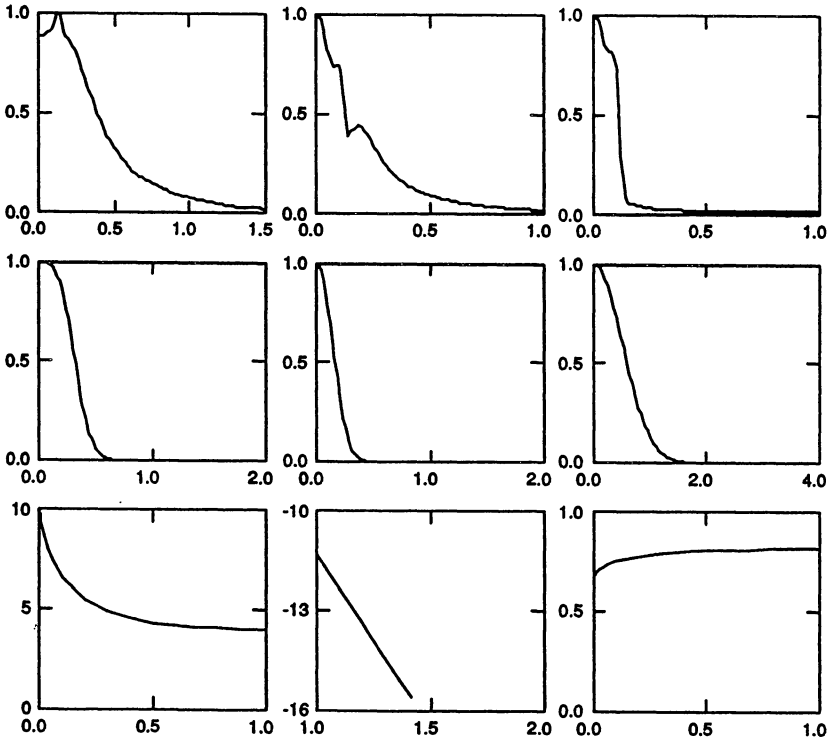

Fig. 5. continued

T = 6000 P = 0.01 Δz = 5000 v_T = 5
m = 7.890E-06 S^{23}_{max} = 5.3E-06 n_H (c) = 6.6E+09 n_H (s) = 6.7E+09
τ(L.c.) = 5.94E+00 τ(B.c.) = 4.00E-06 n_e (c) = 4.8E+09 n_e (s) = 4.7E+09

hydrogen lines	LL	UL	τ	I_{max}	E_{tot}	FWHM
	1	2	6.38E+04	1.80E-08	1.52E+04	0.45
	1	3	1.02E+04	7.66E-11	4.82E+01	0.24
	1	4	3.56E+03	1.61E-11	1.00E+01	0.21
	2	3	1.62E-01	4.65E-07	1.44E+04	0.42
	2	4	2.24E-02	3.57E-08	1.47E+03	0.30
	3	4	2.39E-03	3.85E-08	4.08E+02	1.17
	2	5	7.50E-03	1.11E-08	5.15E+02	0.27
	2	6	3.51E-03	6.75E-09	3.32E+02	0.26
	2	7	1.95E-03	3.37E-09	1.73E+02	0.25

T = 6000 P = 0.05 Δz = 5000 v_T = 5
m = 4.847E-05 S^{23}_{max} = 5.4E-06 n_H (c) = 4.1E+10 n_H (s) = 4.0E+10
τ(L.c.) = 8.00E+01 τ(B.c.) = 4.24E-05 n_e (c) = 1.5E+10 n_e (s) = 1.6E+10

hydrogen lines	LL	UL	τ	I_{max}	E_{tot}	FWHM
	1	2	8.60E+05	1.56E-08	2.72E+04	0.84
	1	3	1.38E+05	8.19E-11	8.07E+01	0.29
	1	4	4.79E+04	1.63E-11	1.17E+01	0.24
	2	3	1.72E+00	3.00E-06	1.14E+05	0.53
	2	4	2.37E-01	3.53E-07	1.49E+04	0.32
	3	4	3.09E-02	4.17E-07	4.43E+03	1.17
	2	5	7.94E-02	1.16E-07	5.39E+03	0.27
	2	6	3.71E-02	7.02E-08	3.43E+03	0.26
	2	7	2.07E-02	3.50E-08	1.77E+03	0.25

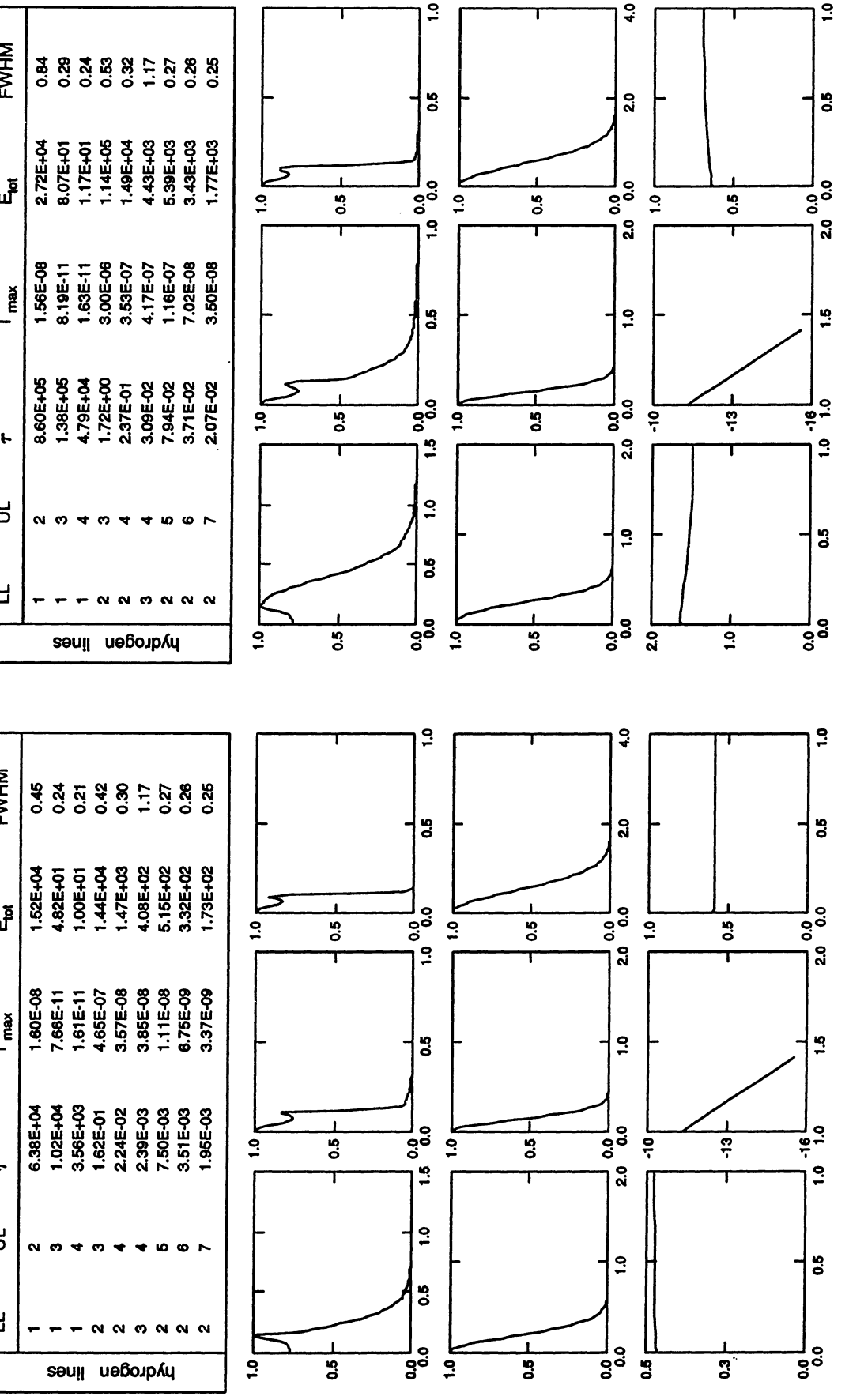

Fig. 5. continued

1993A&AS...99..513G

T = 6000 P = 0.20 Δz = 5000 v_T = 5
m = 2.320E-04 S^{23}_{max} = 5.5E-06 n_H (c) = 2.0E+11 n_H (s) = 1.8E+11
τ(L.c.) = 5.34E+02 τ(B.c.) = 1.19E-04 n_e (c) = 2.4E+10 n_e (s) = 4.0E+10

hydrogen lines	LL	UL	τ	I_{max}	E_{tot}	FWHM
	1	2	5.74E+06	1.46E-08	2.81E+04	0.81
	1	3	9.20E+05	8.81E-11	1.25E+02	0.46
	1	4	3.20E+05	1.70E-11	1.35E+01	0.23
	2	3	4.83E+00	4.39E-06	2.16E+05	0.69
	2	4	6.69E-01	9.09E-07	4.08E+04	0.34
	3	4	1.13E-01	1.17E-06	1.26E+04	1.19
	2	5	2.24E-01	3.24E-07	1.53E+04	0.28
	2	6	1.05E-01	1.98E-07	9.74E+03	0.26
	2	7	5.82E-02	9.90E-08	5.02E+03	0.25

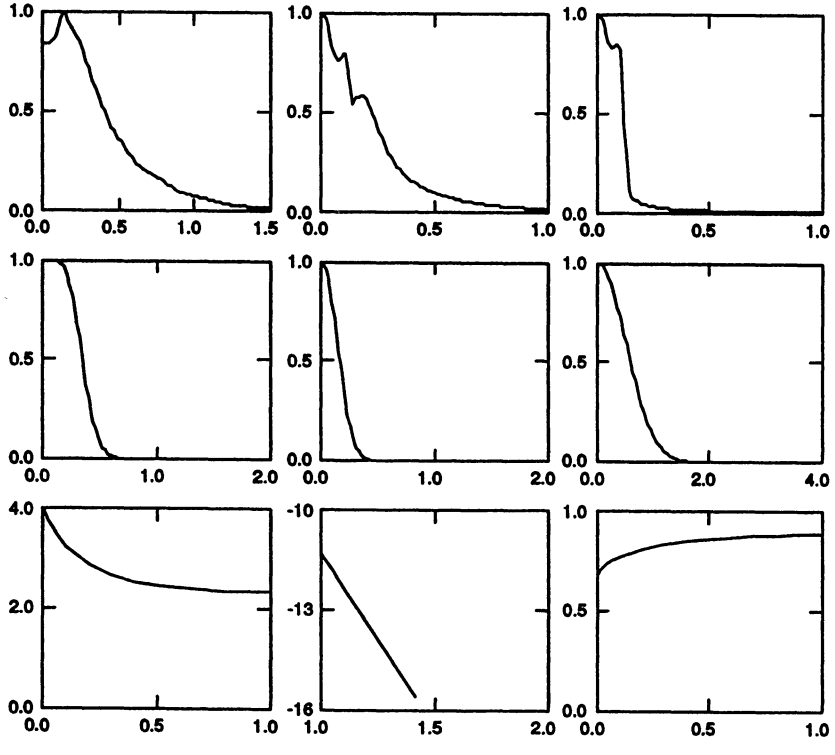

T = 6000 P = 1.00 Δz = 5000 v_T = 5
m = 1.253E-03 S^{23}_{max} = 7.3E-06 n_H (c) = 1.1E+12 n_H (s) = 1.0E+12
τ(L.c.) = 3.19E+03 τ(B.c.) = 3.19E-04 n_e (c) = 4.5E+10 n_e (s) = 1.0E+11

hydrogen lines	LL	UL	τ	I_{max}	E_{tot}	FWHM
	1	2	3.43E+07	1.39E-08	2.69E+04	0.77
	1	3	5.50E+06	9.61E-11	1.58E+02	0.26
	1	4	1.91E+06	1.81E-11	2.14E+01	0.23
	2	3	1.29E+01	6.03E-06	3.52E+05	0.85
	2	4	1.78E+00	1.93E-06	9.95E+04	0.40
	3	4	4.39E-01	3.53E-06	3.97E+04	1.26
	2	5	5.97E-01	8.32E-07	4.14E+04	0.30
	2	6	2.79E-01	4.91E-07	2.48E+04	0.27
	2	7	1.55E-01	2.59E-07	1.33E+04	0.25

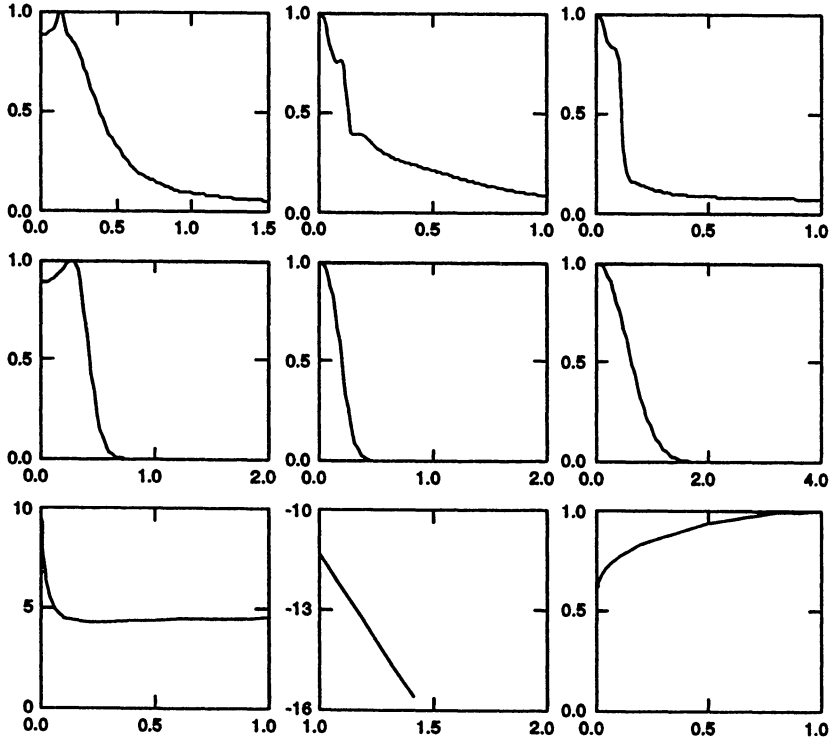

Fig. 5. continued

T = 8000 P = 0.01 Δz = 200 v_T = 5

m = 2.276E-07 S^{23}_{max} = 5.3E-06 n_H (c) = 4.8E+09 n_H (s) = 4.8E+09

τ(L.c.) = 1.28E-01 τ(B.c.) = 7.01E-08 n_e (c) = 3.8E+09 n_e (s) = 3.8E+09

hydrogen lines

LL	UL	τ	I_{max}	E_{tot}	FWHM
1	2	1.22E+03	1.36E-08	7.58E+03	0.28
1	3	1.95E+02	7.75E-11	4.02E+01	0.20
1	4	6.79E+01	1.65E-11	8.36E+00	0.17
2	3	2.52E-03	8.16E-09	2.78E+02	0.46
2	4	3.49E-04	6.02E-10	2.78E+01	0.34
3	4	3.86E-05	6.42E-10	7.66E+00	1.31
2	5	1.17E-04	1.82E-10	9.54E+00	0.30
2	6	5.46E-05	1.06E-10	5.96E+00	0.29
2	7	3.04E-05	5.25E-11	3.11E+00	0.28

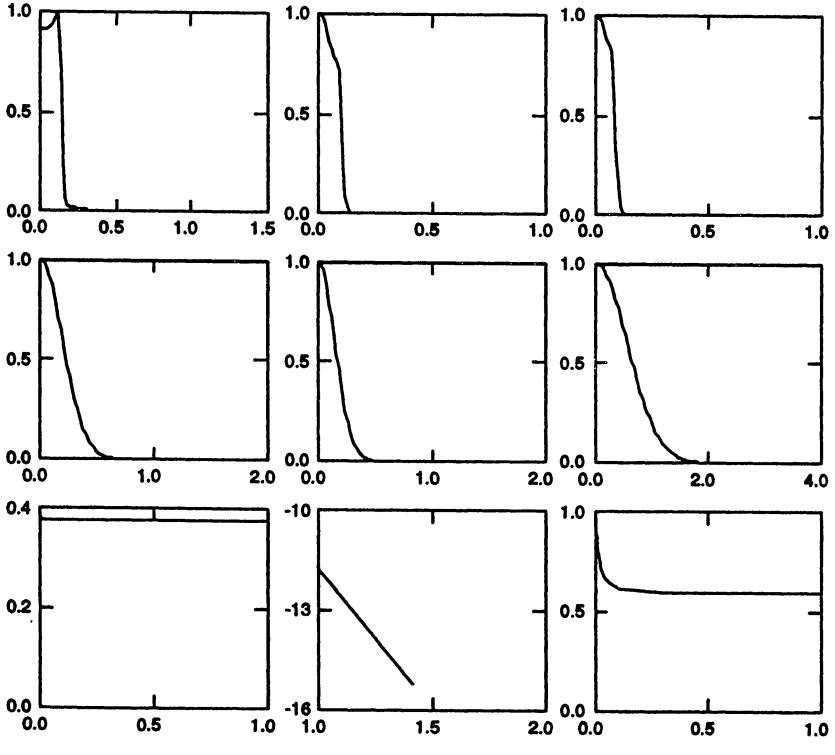

T = 8000 P = 0.05 Δz = 200 v_T = 5

m = 1.319E-06 S^{23}_{max} = 5.4E-06 n_H (c) = 2.8E+10 n_H (s) = 2.8E+10

τ(L.c.) = 1.65E+00 τ(B.c.) = 1.06E-06 n_e (c) = 1.5E+10 n_e (s) = 1.4E+10

hydrogen lines

LL	UL	τ	I_{max}	E_{tot}	FWHM
1	2	1.58E+04	1.55E-08	1.11E+04	0.34
1	3	2.53E+03	7.77E-11	4.90E+01	0.25
1	4	8.78E+02	1.66E-11	1.06E+01	0.22
2	3	3.83E-02	1.19E-07	4.06E+03	0.46
2	4	5.30E-03	8.73E-09	4.02E+02	0.34
3	4	5.73E-04	9.34E-09	1.11E+02	1.31
2	5	1.77E-03	2.66E-09	1.37E+02	0.30
2	6	8.29E-04	1.55E-09	8.50E+01	0.29
2	7	4.61E-04	7.54E-10	4.31E+01	0.28

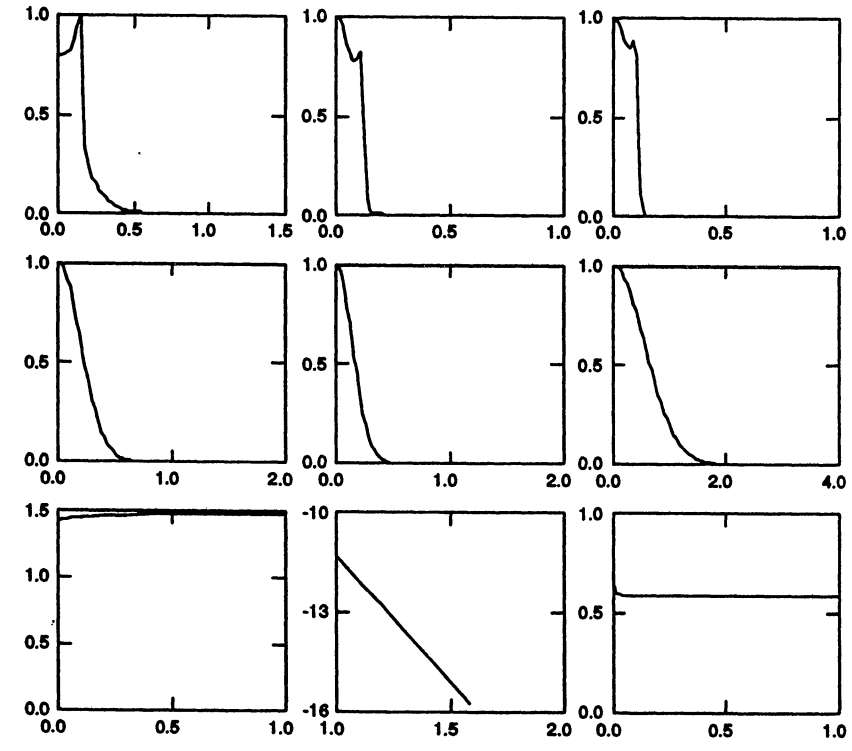

Fig. 5. continued

T = 8000 P = 0.20 Δz = 200 v_T = 5
m = 5.973E-06 S^{23}_{max} = 5.5E-06 n_H (c) = 1.2E+11 n_H (s) = 1.3E+11
τ(L.c.) = 1.05E+01 τ(B.c.) = 8.77E-06 n_e (c) = 4.4E+10 n_e (s) = 3.8E+10

hydrogen lines	LL	UL	τ	I_{max}	E_{tot}	FWHM
	1	2	1.00E+05	1.97E-08	1.96E+04	0.52
	1	3	1.61E+04	8.23E-11	6.27E+01	0.28
	1	4	5.58E+03	1.88E-11	1.30E+01	0.25
	2	3	3.16E-01	9.01E-07	3.21E+04	0.49
	2	4	4.37E-02	7.10E-08	3.28E+03	0.34
	3	4	5.04E-03	7.73E-08	9.21E+02	1.31
	2	5	1.46E-02	2.17E-08	1.12E+03	0.30
	2	6	6.83E-03	1.22E-08	6.67E+02	0.29
	2	7	3.80E-03	5.90E-09	3.34E+02	0.28

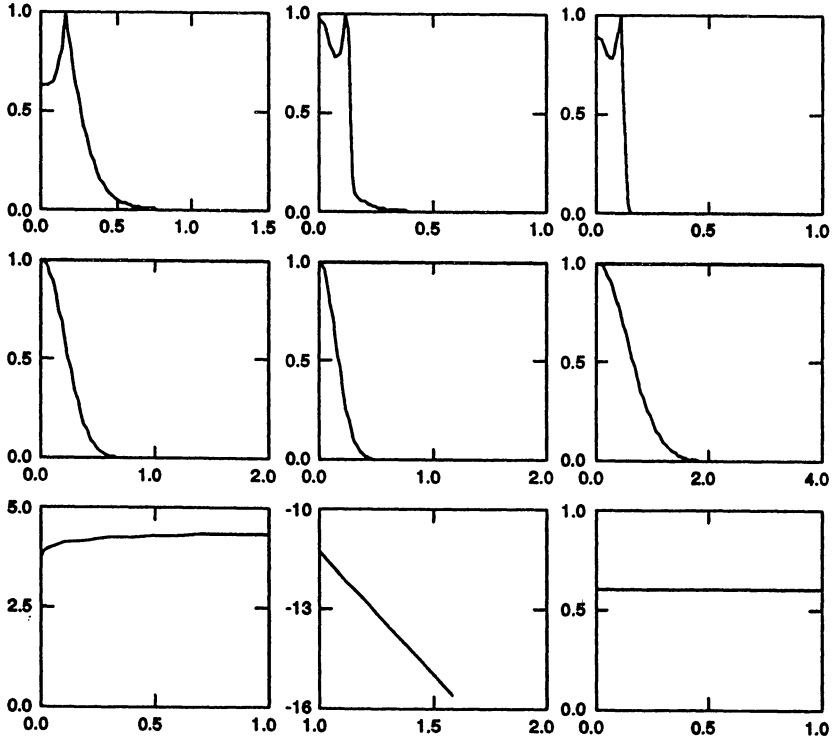

T = 8000 P = 1.00 Δz = 200 v_T = 5
m = 3.202E-05 S^{23}_{max} = 6.1E-06 n_H (c) = 6.7E+11 n_H (s) = 7.3E+11
τ(L.c.) = 6.44E+01 τ(B.c.) = 1.15E-04 n_e (c) = 1.7E+11 n_e (s) = 1.1E+11

hydrogen lines	LL	UL	τ	I_{max}	E_{tot}	FWHM
	1	2	6.15E+05	3.41E-08	4.66E+04	0.77
	1	3	9.86E+04	2.40E-10	1.55E+02	0.31
	1	4	3.43E+04	4.30E-11	2.28E+01	0.27
	2	3	4.15E+00	4.75E-06	2.52E+05	0.75
	2	4	5.74E-01	8.40E-07	4.18E+04	0.38
	3	4	1.05E-01	1.12E-06	1.35E+04	1.34
	2	5	1.92E-01	2.88E-07	1.52E+04	0.31
	2	6	8.98E-02	1.51E-07	8.36E+03	0.29
	2	7	5.00E-02	7.61E-08	4.32E+03	0.28

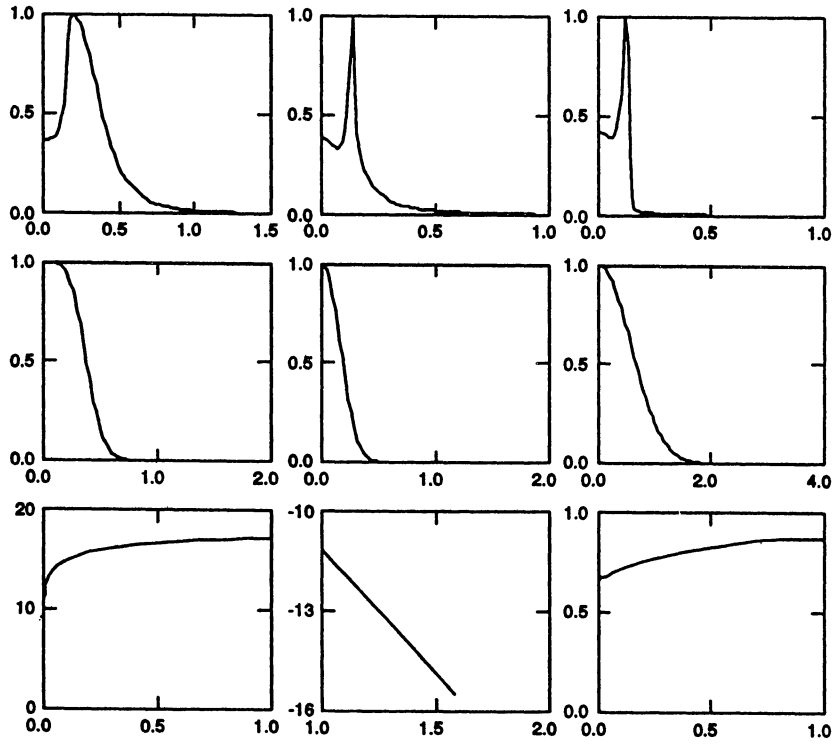

Fig. 5. continued

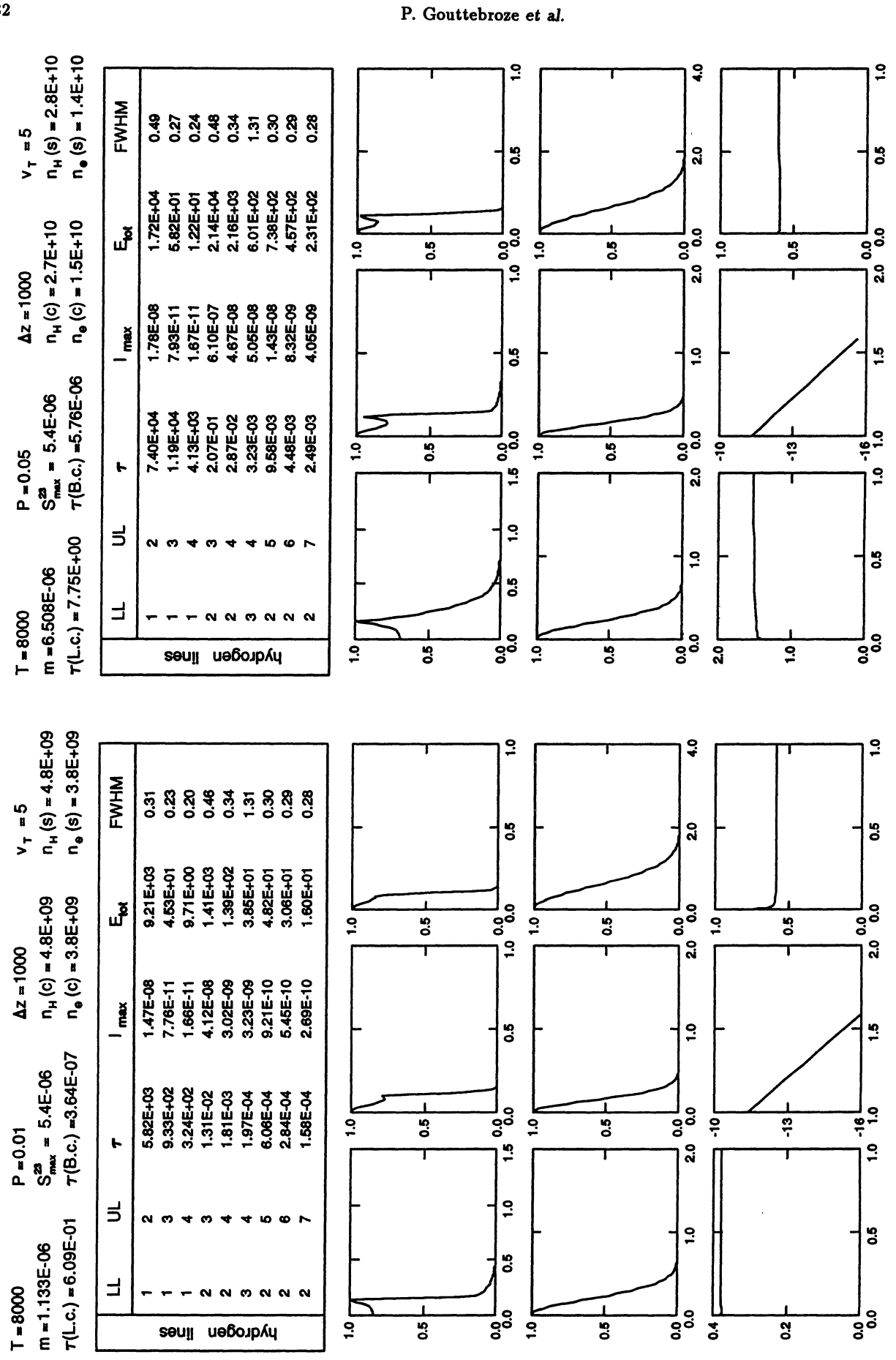

hydrogen lines	LL	UL	τ	I_{max}	E_{tot}	FWHM
	1	2	5.82E+03	1.47E-08	9.21E+03	0.31
	1	3	9.33E+02	7.76E-11	4.53E+01	0.23
	1	4	3.24E+02	1.66E-11	9.71E+00	0.20
	2	3	1.31E-02	4.12E-08	1.41E+03	0.46
	2	4	1.81E-03	3.02E-09	1.39E+02	0.34
	3	4	1.97E-04	3.23E-09	3.85E+01	1.31
	2	5	6.06E-04	9.21E-10	4.82E+01	0.30
	2	6	2.84E-04	5.45E-10	3.06E+01	0.29
	2	7	1.58E-04	2.69E-10	1.60E+01	0.28

hydrogen lines	LL	UL	τ	I_{max}	E_{tot}	FWHM
	1	2	7.40E+04	1.78E-08	1.72E+04	0.49
	1	3	1.19E+04	7.93E-11	5.82E+01	0.27
	1	4	4.13E+03	1.67E-11	1.22E+01	0.24
	2	3	2.07E-01	6.10E-07	2.14E+04	0.48
	2	4	2.87E-02	4.67E-08	2.16E+03	0.34
	3	4	3.23E-03	5.05E-08	6.01E+02	1.31
	2	5	9.58E-03	1.43E-08	7.38E+02	0.30
	2	6	4.48E-03	8.32E-09	4.57E+02	0.29
	2	7	2.49E-03	4.05E-09	2.31E+02	0.28

Fig. 5. continued

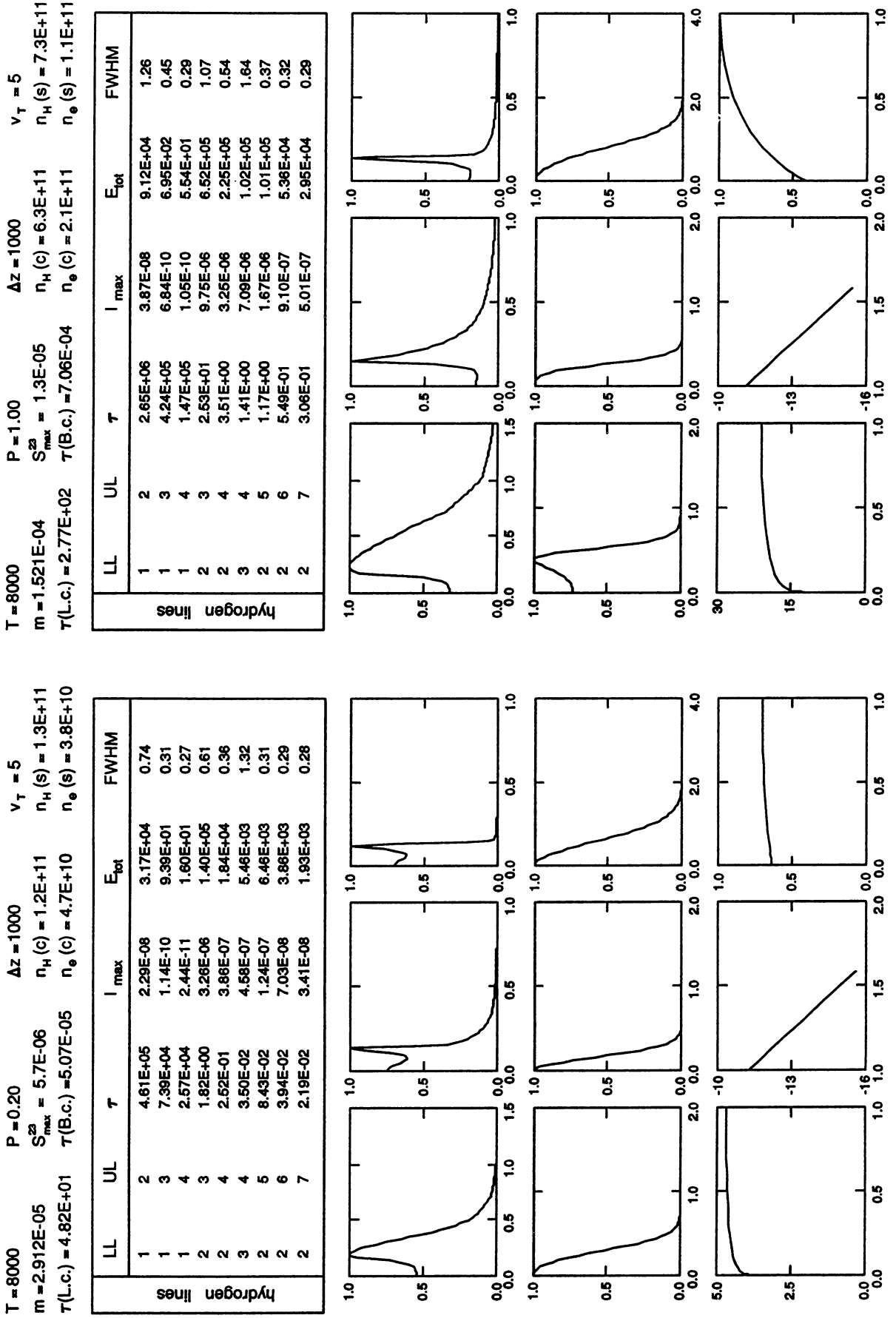

hydrogen lines	LL	UL	τ	I_{max}	E_{tot}	FWHM
	1	2	4.61E+05	2.29E-08	3.17E+04	0.74
	1	3	7.39E+04	1.14E-10	9.39E+01	0.31
	1	4	2.57E+04	2.44E-11	1.60E+01	0.27
	2	3	1.82E+00	3.26E-06	1.40E+05	0.61
	2	4	2.52E-01	3.86E-07	1.84E+04	0.36
	3	4	3.50E-02	4.58E-07	5.46E+03	1.32
	2	5	8.43E-02	1.24E-07	6.46E+03	0.31
	2	6	3.94E-02	7.03E-08	3.86E+03	0.29
	2	7	2.19E-02	3.41E-08	1.93E+03	0.28

hydrogen lines	LL	UL	τ	I_{max}	E_{tot}	FWHM
	1	2	2.65E+06	3.87E-08	9.12E+04	1.26
	1	3	4.24E+05	6.84E-10	6.95E+02	0.45
	1	4	1.47E+05	1.05E-10	5.54E+01	0.29
	2	3	2.53E+01	9.75E-06	6.52E+05	1.07
	2	4	3.51E+00	3.25E-06	2.25E+05	0.54
	3	4	1.41E+00	7.09E-06	1.02E+05	1.64
	2	5	1.17E+00	1.67E-06	1.01E+05	0.37
	2	6	5.49E-01	9.10E-07	5.36E+04	0.32
	2	7	3.06E-01	5.01E-07	2.95E+04	0.29

Fig. 5. continued

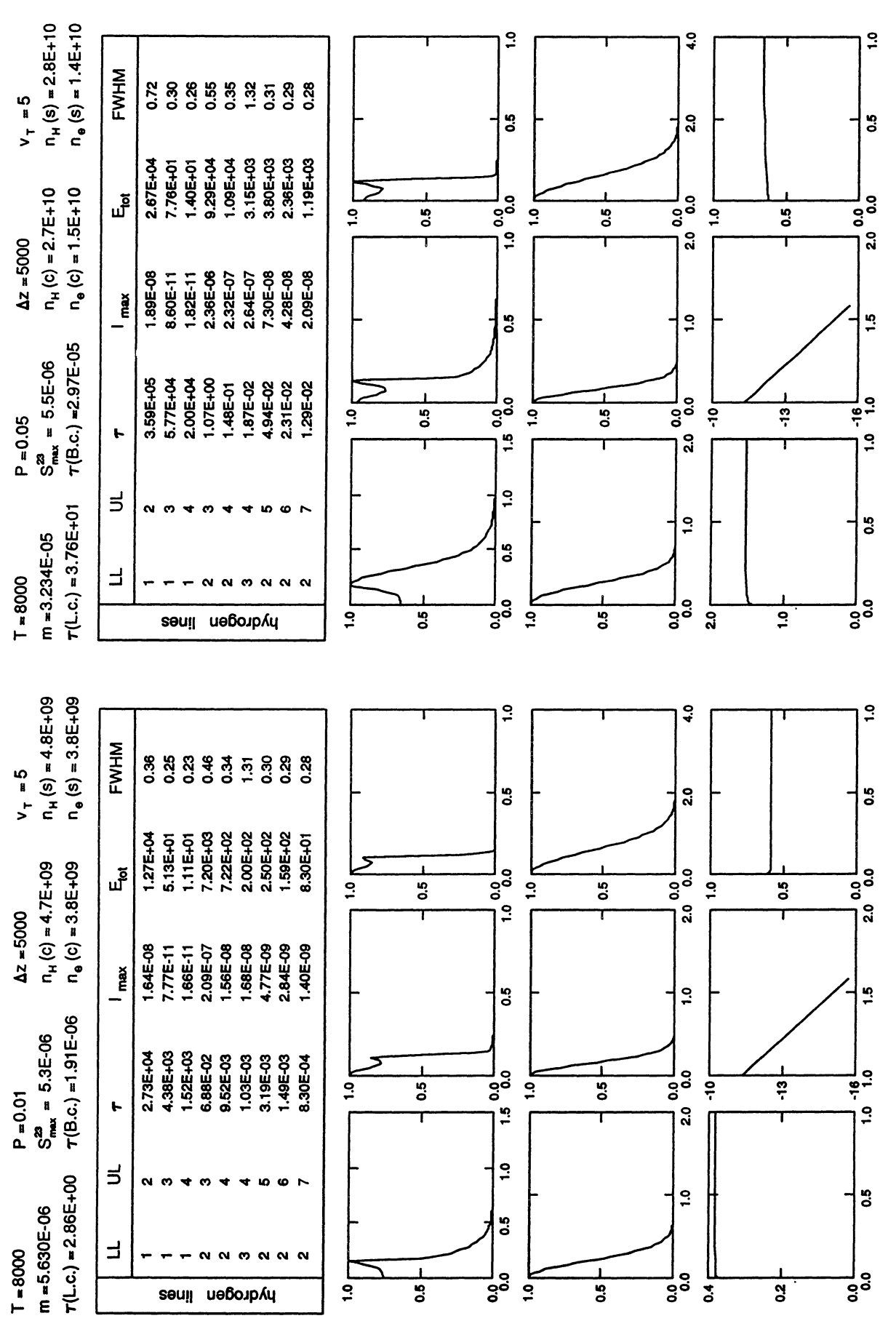

hydrogen lines	LL	UL	τ	I_{max}	E_{tot}	FWHM
	1	2	2.73E+04	1.64E-08	1.27E+04	0.36
	1	3	4.38E+03	7.77E-11	5.13E+01	0.25
	1	4	1.52E+03	1.66E-11	1.11E+01	0.23
	2	3	6.88E-02	2.09E-07	7.20E+03	0.46
	2	4	9.52E-03	1.56E-08	7.22E+02	0.34
	3	4	1.03E-03	1.68E-08	2.00E+02	1.31
	2	5	3.19E-03	4.77E-09	2.50E+02	0.30
	2	6	1.49E-03	2.84E-09	1.59E+02	0.29
	2	7	8.30E-04	1.40E-09	8.30E+01	0.28

hydrogen lines	LL	UL	τ	I_{max}	E_{tot}	FWHM
	1	2	3.59E+05	1.89E-08	2.67E+04	0.72
	1	3	5.77E+04	8.60E-11	7.76E+01	0.30
	1	4	2.00E+04	1.82E-11	1.40E+01	0.26
	2	3	1.07E+00	2.36E-06	9.29E+04	0.55
	2	4	1.48E-01	2.32E-07	1.09E+04	0.35
	3	4	1.87E-02	2.64E-07	3.15E+03	1.32
	2	5	4.94E-02	7.30E-08	3.80E+03	0.31
	2	6	2.31E-02	4.28E-08	2.36E+03	0.29
	2	7	1.29E-02	2.09E-08	1.19E+03	0.28

Fig. 5. continued

T = 8000 P = 0.20 Δz = 5000 v_T = 5
m = 1.383E-04 S^{23}_{max} = 7.4E-06 n_H (c) = 1.1E+11 n_H (s) = 1.3E+11
τ(L.c.) = 2.00E+02 τ(B.c.) = 3.08E-04 n_e (c) = 5.5E+10 n_e (s) = 3.8E+10

hydrogen lines	LL	UL	τ	I_{max}	E_{tot}	FWHM
	1	2	1.91E+06	2.63E-08	5.24E+04	1.03
	1	3	3.07E+05	2.66E-10	2.46E+02	0.39
	1	4	1.07E+05	4.57E-11	2.66E+01	0.29
	2	3	1.11E+01	6.13E-06	3.96E+05	0.94
	2	4	1.53E+00	1.81E-06	1.02E+05	0.43
	3	4	3.76E-01	3.17E-06	3.98E+04	1.40
	2	5	5.13E-01	7.18E-07	3.98E+04	0.33
	2	6	2.40E-01	4.06E-07	2.29E+04	0.30
	2	7	1.33E-01	2.09E-07	1.20E+04	0.28

T = 8000 P = 1.00 Δz = 5000 v_T = 5
m = 7.206E-04 S^{23}_{max} = 2.3E-05 n_H (c) = 6.0E+11 n_H (s) = 7.2E+11
τ(L.c.) = 1.16E+03 τ(B.c.) = 3.33E-03 n_e (c) = 2.5E+11 n_e (s) = 1.1E+11

hydrogen lines	LL	UL	τ	I_{max}	E_{tot}	FWHM
	1	2	1.11E+07	3.97E-08	1.51E+05	2.18
	1	3	1.78E+06	1.41E-09	3.07E+03	0.86
	1	4	6.18E+05	2.58E-10	2.13E+02	0.33
	2	3	1.18E+02	1.81E-05	1.19E+06	1.27
	2	4	1.66E+01	6.79E-06	5.90E+05	0.74
	3	4	1.19E+01	1.09E-05	2.51E+05	2.68
	2	5	5.54E+00	4.14E-06	3.62E+05	0.54
	2	6	2.59E+00	3.03E-06	2.28E+05	0.42
	2	7	1.44E+00	2.18E-06	1.49E+05	0.35

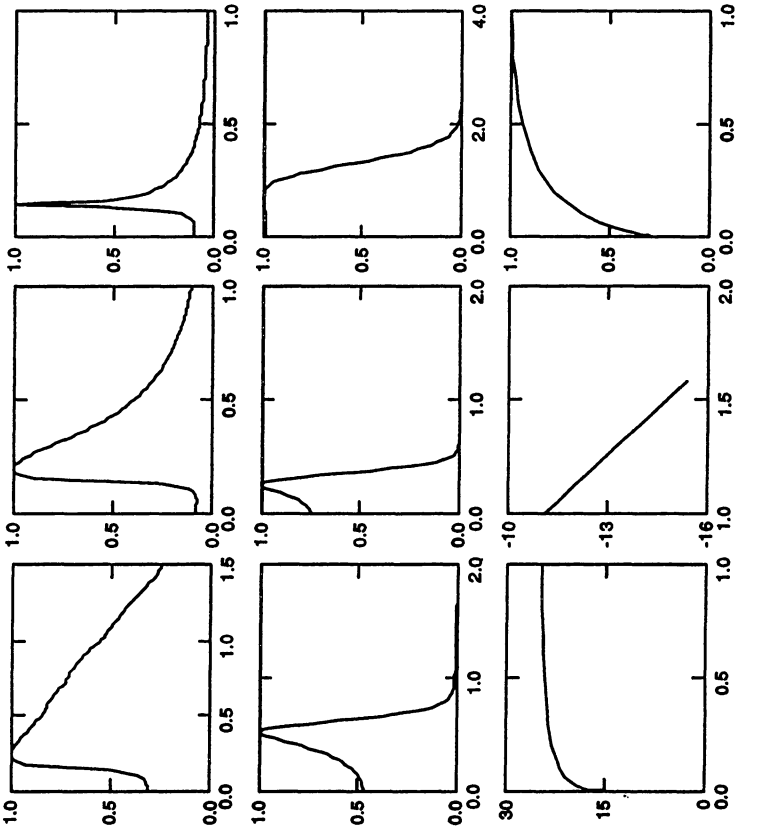

Fig. 5. continued

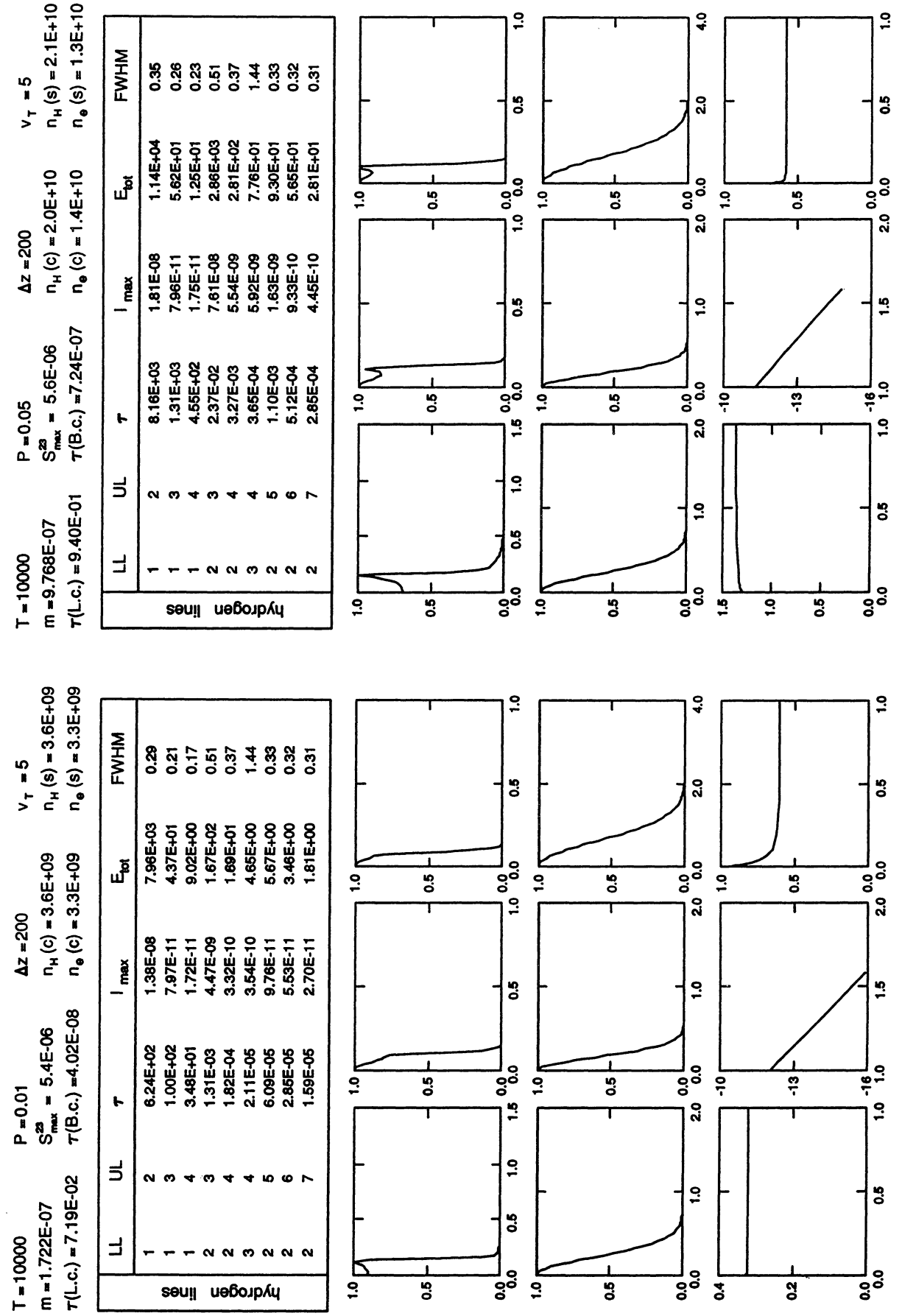

Fig. 5. continued

T = 10000 P = 0.20 Δz = 200 v_T = 5
m = 4.007E-06 S^{23}_{max} = 6.2E-06 n_H (c) = 8.3E+10 n_H (s) = 9.5E+10
τ(L.c.) = 4.15E+00 τ(B.c.) = 1.00E-05 n_e (c) = 5.4E+10 n_e (s) = 4.0E+10

hydrogen lines	LL	UL	τ	I_{max}	E_{tot}	FWHM
	1	2	3.61E+04	4.80E-08	2.41E+04	0.40
	1	3	5.79E+03	2.26E-10	1.02E+02	0.29
	1	4	2.01E+03	5.16E-11	2.45E+01	0.26
	2	3	3.27E-01	9.67E-07	3.79E+04	0.54
	2	4	4.52E-02	7.59E-08	3.86E+03	0.38
	3	4	5.45E-03	8.26E-08	1.08E+03	1.44
	2	5	1.51E-02	2.23E-08	1.27E+03	0.34
	2	6	7.07E-03	1.20E-08	7.21E+02	0.32
	2	7	3.94E-03	5.65E-09	3.52E+02	0.31

T = 10000 P = 1.00 Δz = 200 v_T = 5
m = 1.869E-05 S^{23}_{max} = 8.5E-06 n_H (c) = 3.8E+11 n_H (s) = 5.0E+11
τ(L.c.) = 1.29E+01 τ(B.c.) = 2.27E-04 n_e (c) = 3.0E+11 n_e (s) = 1.7E+11

hydrogen lines	LL	UL	τ	I_{max}	E_{tot}	FWHM
	1	2	1.12E+05	3.23E-07	1.64E+05	0.48
	1	3	1.80E+04	3.36E-09	9.41E+02	0.31
	1	4	6.26E+03	5.47E-10	1.70E+02	0.28
	2	3	7.39E+00	7.06E-06	4.73E+05	0.95
	2	4	1.02E+00	1.70E-06	9.91E+04	0.44
	3	4	2.89E-01	2.53E-06	3.45E+04	1.52
	2	5	3.43E-01	5.64E-07	3.35E+04	0.35
	2	6	1.60E-01	2.73E-07	1.67E+04	0.32
	2	7	8.92E-02	1.41E-07	8.87E+03	0.31

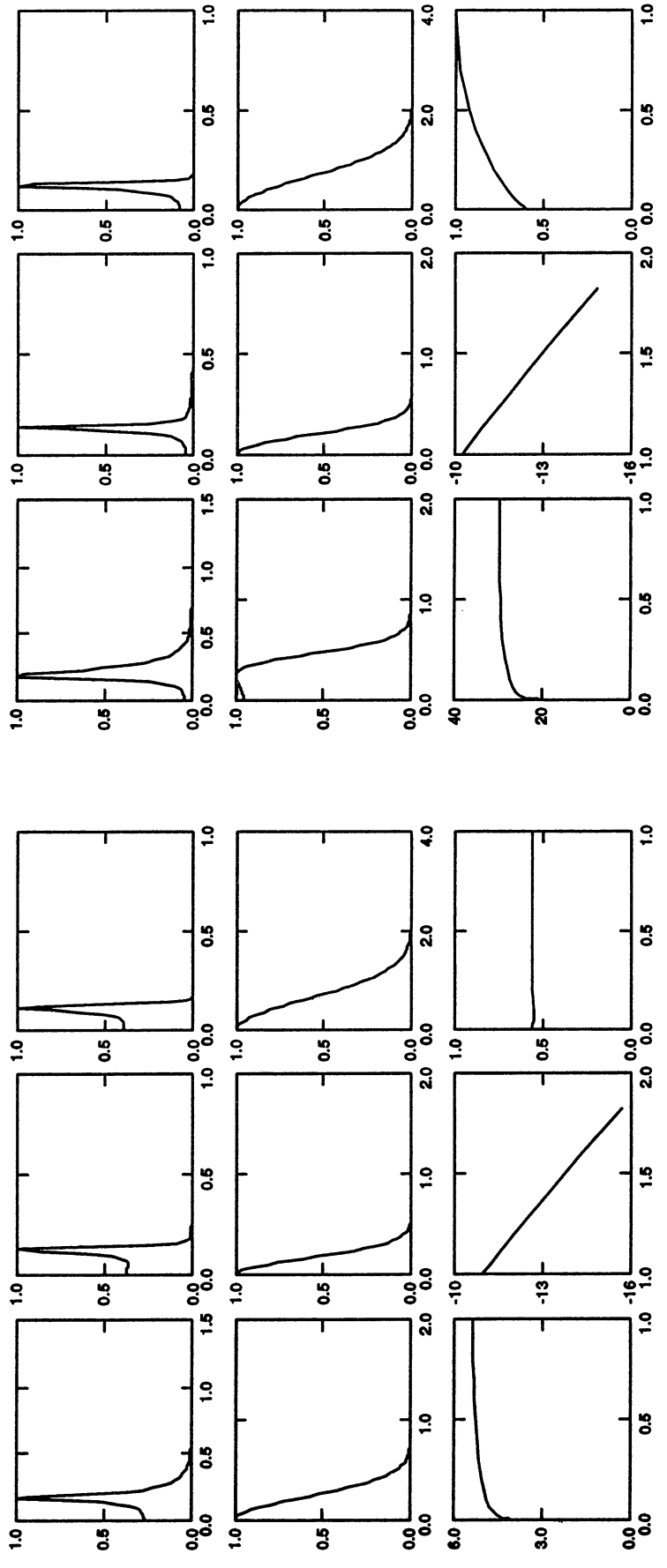

Fig. 5. continued

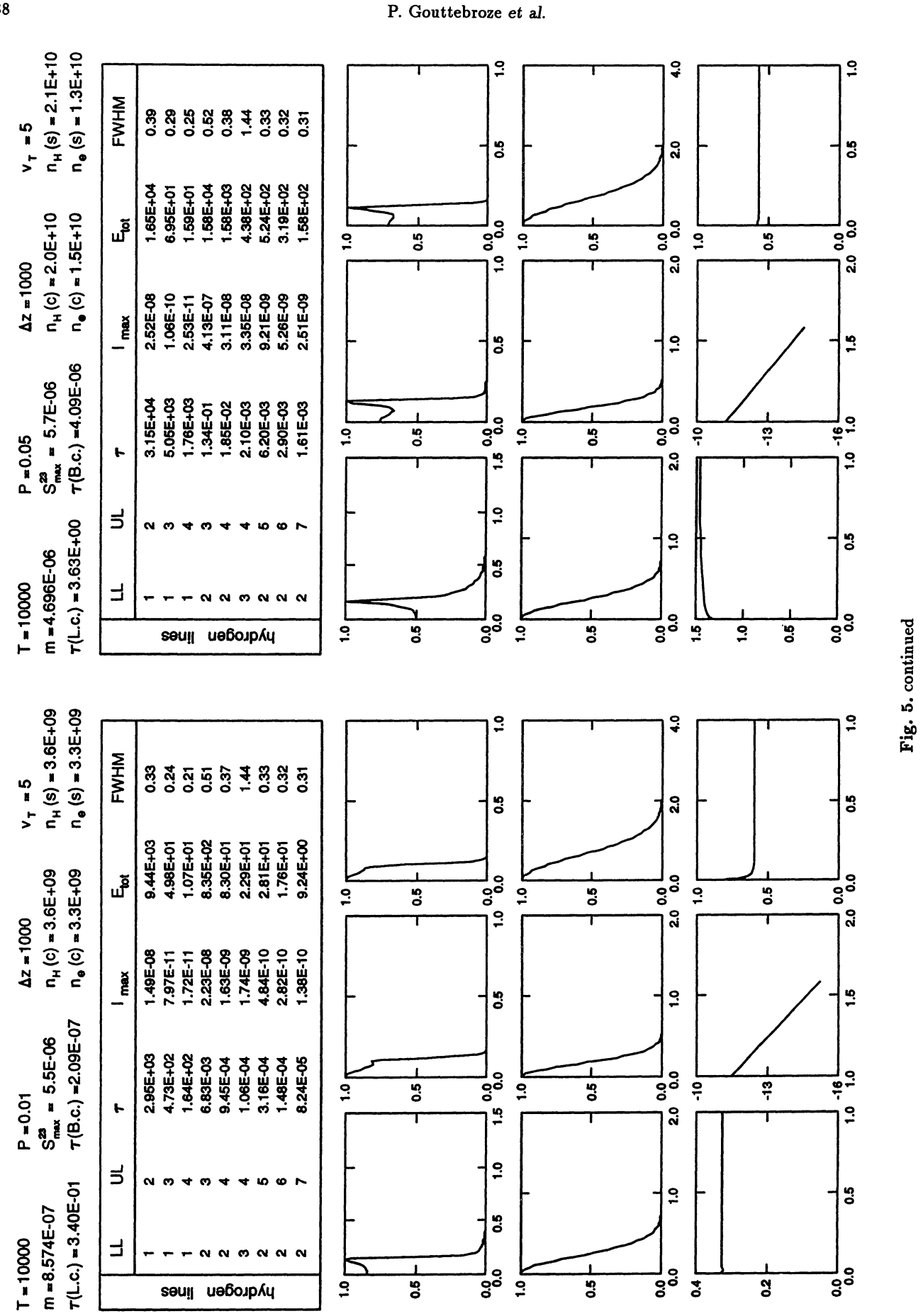

hydrogen lines	LL	UL	τ	I_{max}	E_{tot}	FWHM
	1	2	2.95E+03	1.49E-08	9.44E+03	0.33
	1	3	4.73E+02	7.97E-11	4.98E+01	0.24
	1	4	1.64E+02	1.72E-11	1.07E+01	0.21
	2	3	6.83E-03	2.23E-08	8.35E+02	0.51
	2	4	9.45E-04	1.63E-09	8.30E+01	0.37
	3	4	1.06E-04	1.74E-09	2.29E+01	1.44
	2	5	3.16E-04	4.84E-10	2.81E+01	0.33
	2	6	1.48E-04	2.82E-10	1.76E+01	0.32
	2	7	8.24E-05	1.38E-10	9.24E+00	0.31

hydrogen lines	LL	UL	τ	I_{max}	E_{tot}	FWHM
	1	2	3.15E+04	2.52E-08	1.65E+04	0.39
	1	3	5.05E+03	1.06E-10	6.95E+01	0.29
	1	4	1.76E+03	2.53E-11	1.59E+01	0.25
	2	3	1.34E-01	4.13E-07	1.58E+04	0.52
	2	4	1.85E-02	3.11E-08	1.58E+03	0.38
	3	4	2.10E-03	3.35E-08	4.38E+02	1.44
	2	5	6.20E-03	9.21E-09	5.24E+02	0.33
	2	6	2.90E-03	5.26E-09	3.19E+02	0.32
	2	7	1.61E-03	2.51E-09	1.58E+02	0.31

Fig. 5. continued

T = 10000 P = 0.20 Δz = 1000 v_T = 5
m = 1.850E-05 S^{23}_{max} = 6.5E-06 n_H (c) = 7.6E+10 n_H (s) = 9.3E+10
τ(L.c.) = 1.22E+01 τ(B.c.) = 6.10E-05 n_e (c) = 6.1E+10 n_e (s) = 4.2E+10

Hydrogen lines	LL	UL	τ	I_{max}	E_{tot}	FWHM
	1	2	1.05E+05	9.53E-08	5.25E+04	0.48
	1	3	1.69E+04	5.48E-10	1.96E+02	0.31
	1	4	5.88E+03	1.12E-10	4.24E+01	0.27
	2	3	2.00E+00	3.61E-06	1.75E+05	0.68
	2	4	2.76E-01	4.39E-07	2.31E+04	0.39
	3	4	4.16E-02	5.25E-07	6.92E+03	1.45
	2	5	9.24E-02	1.37E-07	7.87E+03	0.34
	2	6	4.32E-02	7.38E-08	4.46E+03	0.32
	2	7	2.40E-02	3.52E-08	2.20E+03	0.31

T = 10000 P = 1.00 Δz = 1000 v_T = 5
m = 8.789E-05 S^{23}_{max} = 1.9E-05 n_H (c) = 3.6E+11 n_H (s) = 4.9E+11
τ(L.c.) = 3.37E+01 τ(B.c.) = 9.57E-04 n_e (c) = 3.2E+11 n_e (s) = 1.8E+11

Hydrogen lines	LL	UL	τ	I_{max}	E_{tot}	FWHM
	1	2	2.92E+05	5.11E-07	4.01E+05	0.62
	1	3	4.69E+04	1.07E-08	3.50E+03	0.33
	1	4	1.63E+04	1.76E-09	4.55E+02	0.29
	2	3	3.10E+01	1.42E-05	1.03E+06	1.21
	2	4	4.32E+00	4.70E-06	3.82E+05	0.63
	3	4	2.54E+00	8.65E-06	1.53E+05	2.05
	2	5	1.45E+00	2.44E-06	1.68E+05	0.42
	2	6	6.76E-01	1.29E-06	8.53E+04	0.35
	2	7	3.77E-01	7.29E-07	4.78E+04	0.33

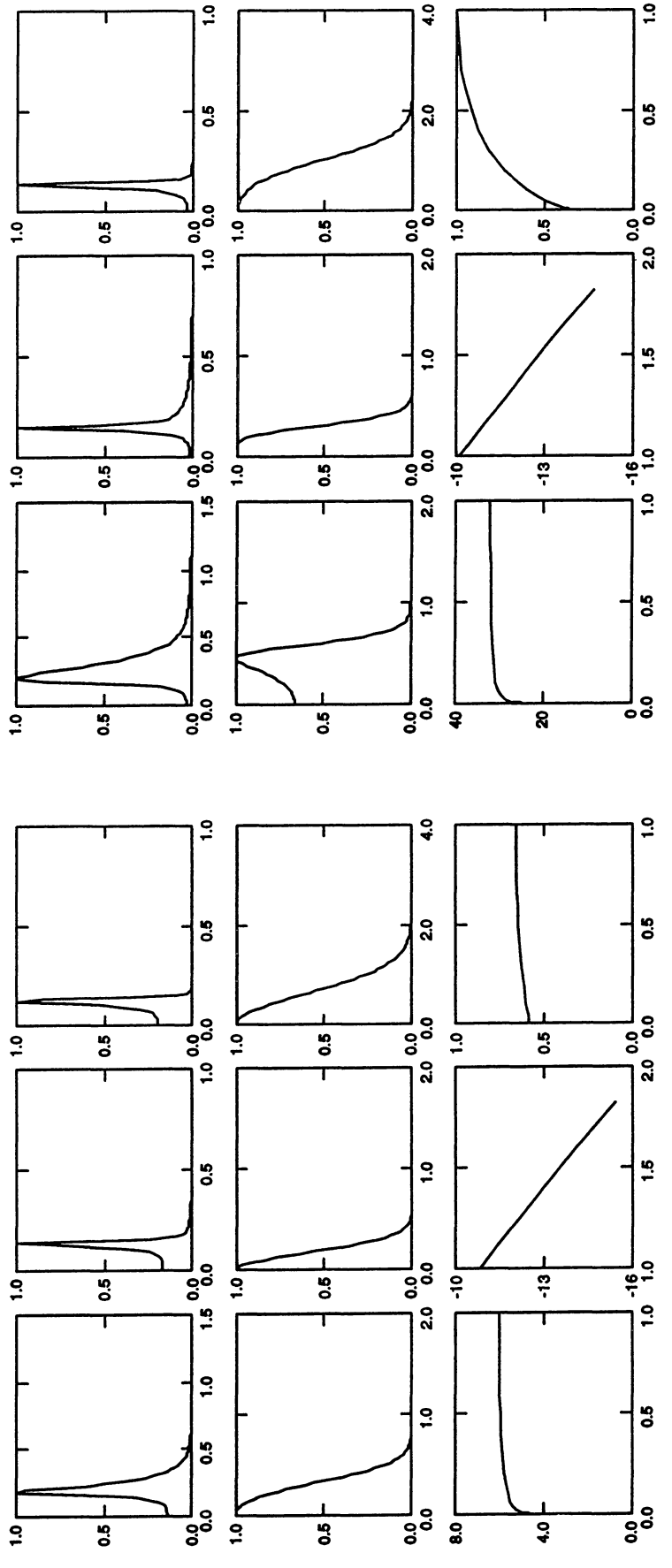

Fig. 5. continued

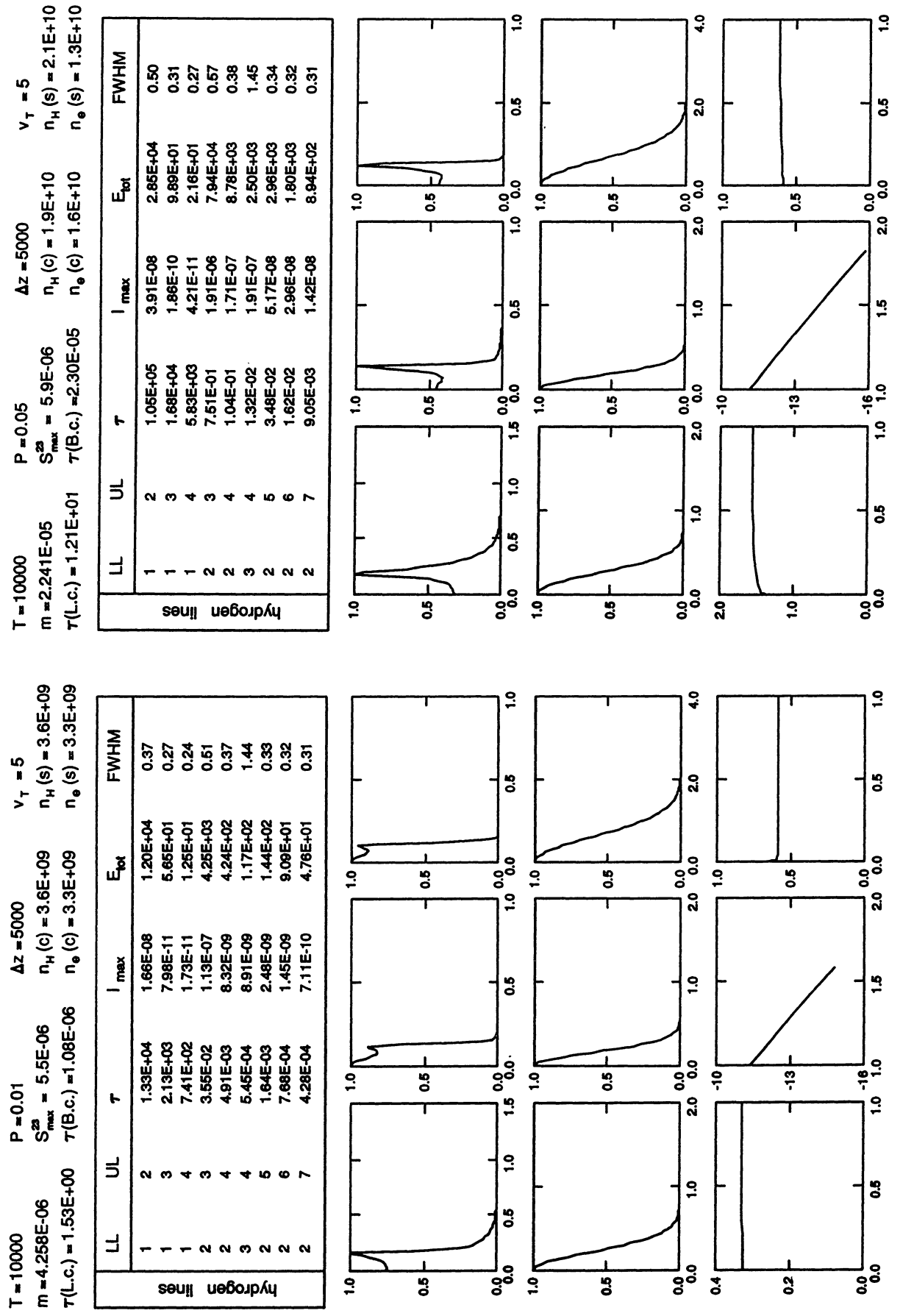

hydrogen lines	LL	UL	τ	I_{max}	E_{tot}	FWHM
	1	2	1.33E+04	1.66E-08	1.20E+04	0.37
	1	3	2.13E+03	7.98E-11	5.65E+01	0.27
	1	4	7.41E+02	1.73E-11	1.25E+01	0.24
	2	3	3.55E-02	1.13E-07	4.25E+03	0.51
	2	4	4.91E-03	8.32E-09	4.24E+02	0.37
	3	4	5.45E-04	8.91E-09	1.17E+02	1.44
	2	5	1.64E-03	2.48E-09	1.44E+02	0.33
	2	6	7.68E-04	1.45E-09	9.09E+01	0.32
	2	7	4.28E-04	7.11E-10	4.76E+01	0.31

hydrogen lines	LL	UL	τ	I_{max}	E_{tot}	FWHM
	1	2	1.05E+05	3.91E-08	2.85E+04	0.50
	1	3	1.68E+04	1.86E-10	9.89E+01	0.31
	1	4	5.83E+03	4.21E-11	2.16E+01	0.27
	2	3	7.51E-01	1.91E-06	7.94E+04	0.57
	2	4	1.04E-01	1.71E-07	8.78E+03	0.38
	3	4	1.32E-02	1.91E-07	2.50E+03	1.45
	2	5	3.48E-02	5.17E-08	2.96E+03	0.34
	2	6	1.62E-02	2.96E-08	1.80E+03	0.32
	2	7	9.05E-03	1.42E-08	8.94E+02	0.31

Fig. 5. continued

T = 10000 P = 0.20 Δz = 5000 v_T = 5
m = 8.761E-05 S^{23}_{max} = 7.9E-06 n_H (c) = 7.3E+10 n_H (s) = 9.1E+10
τ(L.c.) = 3.33E+01 τ(B.c.) = 3.22E-04 n_e (c) = 6.5E+10 n_e (s) = 4.4E+10

hydrogen lines	LL	UL	τ	I_{max}	E_{tot}	FWHM
	1	2	2.89E+05	1.71E-07	1.28E+05	0.61
	1	3	4.63E+04	1.64E-09	5.49E+02	0.32
	1	4	1.61E+04	2.92E-10	8.95E+01	0.29
	2	3	1.05E+01	6.52E-06	4.60E+05	1.02
	2	4	1.45E+00	1.86E-06	1.14E+05	0.47
	3	4	3.60E-01	3.15E-06	4.36E+04	1.54
	2	5	4.87E-01	7.04E-07	4.28E+04	0.36
	2	6	2.27E-01	3.79E-07	2.35E+04	0.33
	2	7	1.27E-01	1.90E-07	1.21E+04	0.31

T = 10000 P = 1.00 Δz = 5000 v_T = 5
m = 4.250E-04 S^{23}_{max} = 3.0E-05 n_H (c) = 3.5E+11 n_H (s) = 4.8E+11
τ(L.c.) = 8.77E+01 τ(B.c.) = 3.46E-03 n_e (c) = 3.3E+11 n_e (s) = 1.9E+11

hydrogen lines	LL	UL	τ	I_{max}	E_{tot}	FWHM
	1	2	7.62E+05	6.37E-07	8.61E+05	0.87
	1	3	1.22E+05	2.35E-08	1.24E+04	0.36
	1	4	4.25E+04	4.67E-09	1.18E+03	0.30
	2	3	1.11E+02	2.36E-05	1.69E+06	1.39
	2	4	1.56E+01	8.77E-06	8.33E+05	0.81
	3	4	1.47E+01	1.07E-05	2.82E+05	3.05
	2	5	5.23E+00	5.08E-06	4.84E+05	0.59
	2	6	2.45E+00	3.64E-06	2.99E+05	0.45
	2	7	1.36E+00	2.61E-06	1.95E+05	0.38

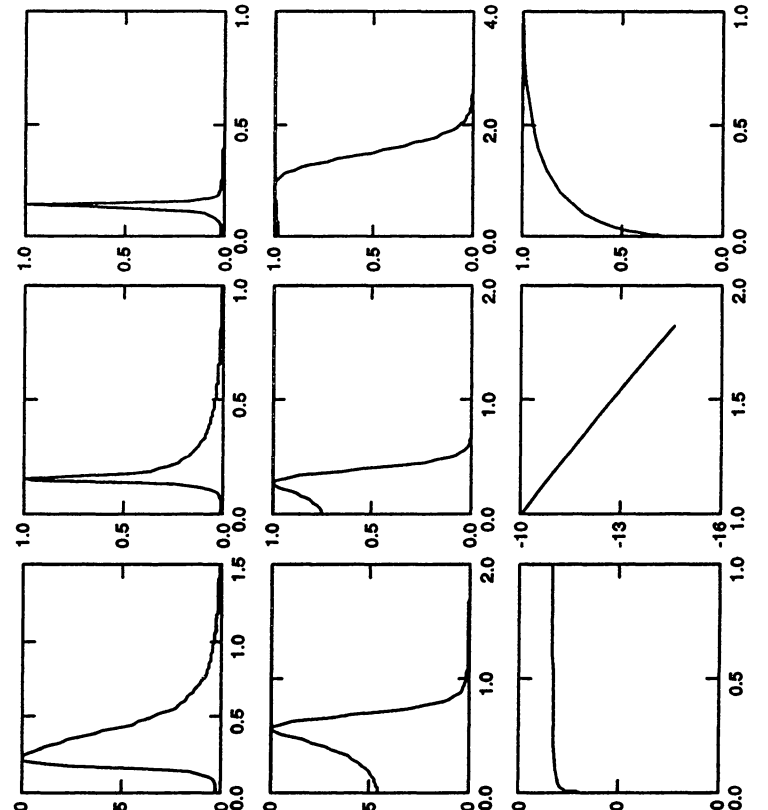

Fig. 5. continued

1993A&AS...99..513G

T = 15000 P = 0.01 Δz = 5000 v_T = 5
m = 2.670E-06 S^{23}_{max} = 6.3E-06 n_H (c) = 2.2E+09 n_H (s) = 2.3E+09
τ(L.c.) = 3.77E-01 τ(B.c.) = 4.18E-07 n_e (c) = 2.4E+09 n_e (s) = 2.3E+09

hydrogen lines	LL	UL	τ	I_{max}	E_{tot}	FWHM
	1	2	2.73E+03	2.46E-08	1.42E+04	0.39
	1	3	4.39E+02	1.13E-10	8.02E+01	0.29
	1	4	1.52E+02	2.70E-11	1.90E+01	0.25
	2	3	1.14E-02	4.00E-08	1.80E+03	0.61
	2	4	1.58E-03	2.91E-09	1.79E+02	0.45
	3	4	1.91E-04	3.11E-09	4.91E+01	1.73
	2	5	5.29E-04	8.30E-10	5.88E+01	0.40
	2	6	2.48E-04	4.69E-10	3.63E+01	0.38
	2	7	1.38E-04	2.26E-10	1.93E+01	0.37

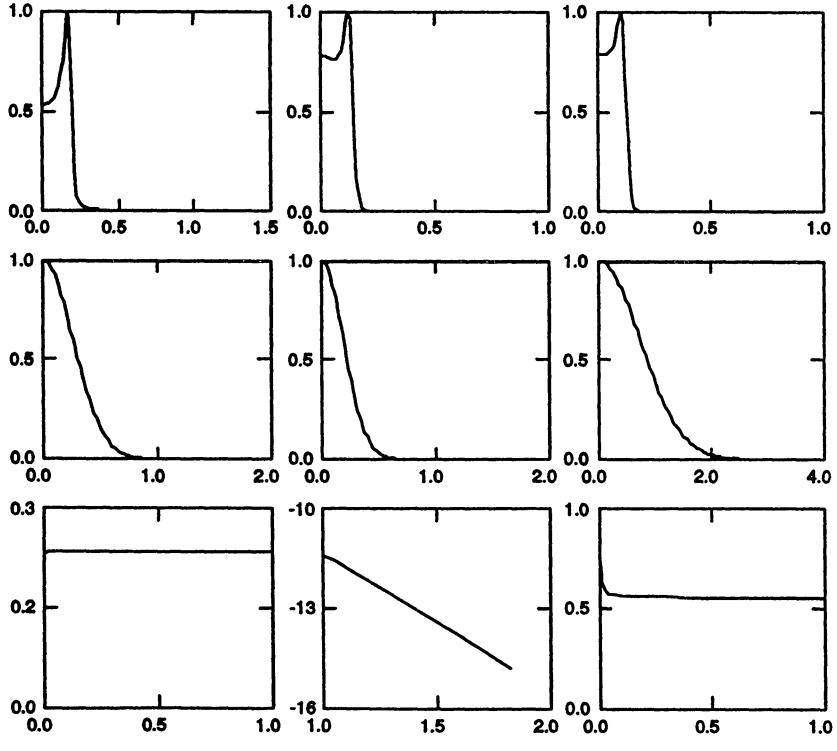

T = 15000 P = 0.05 Δz = 5000 v_T = 5
m = 1.326E-05 S^{23}_{max} = 7.2E-06 n_H (c) = 1.1E+10 n_H (s) = 1.2E+10
τ(L.c.) = 1.33E+00 τ(B.c.) = 9.62E-06 n_e (c) = 1.2E+10 n_e (s) = 1.1E+10

hydrogen lines	LL	UL	τ	I_{max}	E_{tot}	FWHM
	1	2	9.66E+03	1.46E-07	5.00E+04	0.42
	1	3	1.55E+03	6.97E-10	2.87E+02	0.32
	1	4	5.39E+02	1.66E-10	7.71E+01	0.28
	2	3	2.63E-01	8.54E-07	3.98E+04	0.63
	2	4	3.63E-02	6.52E-08	3.98E+03	0.45
	3	4	4.67E-03	7.07E-08	1.11E+03	1.73
	2	5	1.22E-02	1.84E-08	1.26E+03	0.40
	2	6	5.68E-03	1.01E-08	7.35E+02	0.38
	2	7	3.17E-03	4.63E-09	3.56E+02	0.37

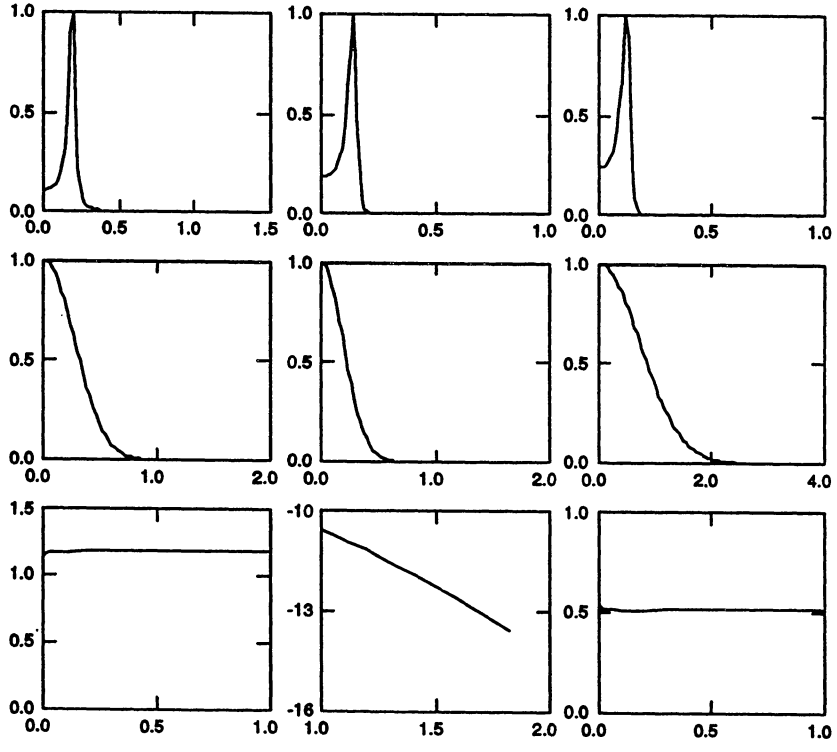

Fig. 5. continued

T = 15000 P = 0.20 Δz = 5000 v_T = 5
m = 5.255E-05 S^{23}_{max} = 9.1E-06 n_H (c) = 4.4E+10 n_H (s) = 4.6E+10
τ(L.c.) = 2.61E+00 τ(B.c.) = 1.18E-04 n_e (c) = 4.8E+10 n_e (s) = 4.6E+10

hydrogen lines

LL	UL	τ	I_{max}	E_{tot}	FWHM
1	2	1.89E+04	9.29E-07	2.79E+05	0.44
1	3	3.03E+03	6.12E-09	2.02E+03	0.33
1	4	1.05E+03	1.18E-09	4.67E+02	0.29
2	3	3.22E+00	5.02E-06	3.26E+05	0.92
2	4	4.47E-01	7.45E-07	4.81E+04	0.48
3	4	8.69E-02	9.44E-07	1.50E+04	1.75
2	5	1.49E-01	2.26E-07	1.57E+04	0.41
2	6	6.98E-02	1.16E-07	8.44E+03	0.38
2	7	3.89E-02	5.27E-08	3.98E+03	0.37

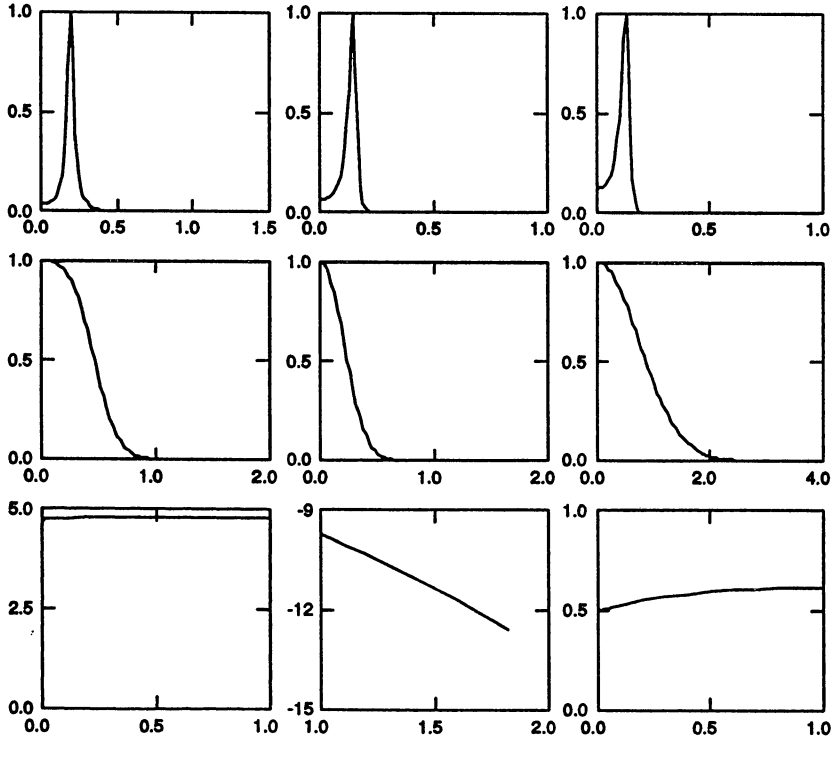

T = 15000 P = 1.00 Δz = 5000 v_T = 5
m = 2.613E-04 S^{23}_{max} = 2.5E-05 n_H (c) = 2.2E+11 n_H (s) = 2.2E+11
τ(L.c.) = 4.39E+00 τ(B.c.) = 1.24E-03 n_e (c) = 2.4E+11 n_e (s) = 2.4E+11

hydrogen lines

LL	UL	τ	I_{max}	E_{tot}	FWHM
1	2	3.18E+04	5.47E-06	1.93E+06	0.46
1	3	5.11E+03	1.37E-07	3.98E+04	0.35
1	4	1.77E+03	2.24E-08	7.51E+03	0.31
2	3	3.35E+01	1.90E-05	1.64E+06	1.46
2	4	4.68E+00	6.19E-06	6.14E+05	0.77
3	4	3.67E+00	9.08E-06	2.10E+05	2.70
2	5	1.57E+00	3.04E-06	2.55E+05	0.51
2	6	7.32E-01	1.52E-06	1.22E+05	0.43
2	7	4.08E-01	8.36E-07	6.62E+04	0.39

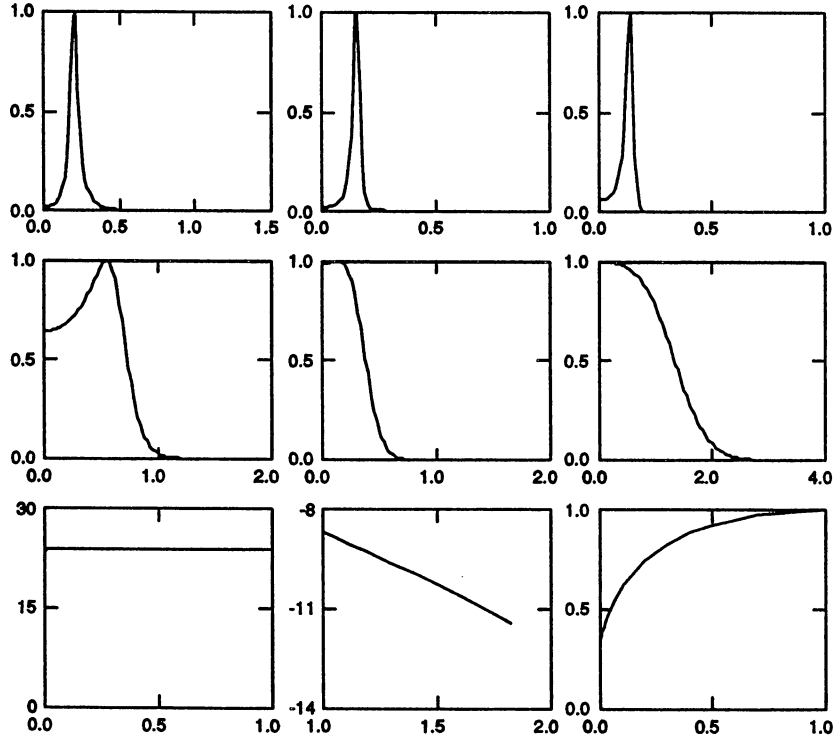

Fig. 5. continued